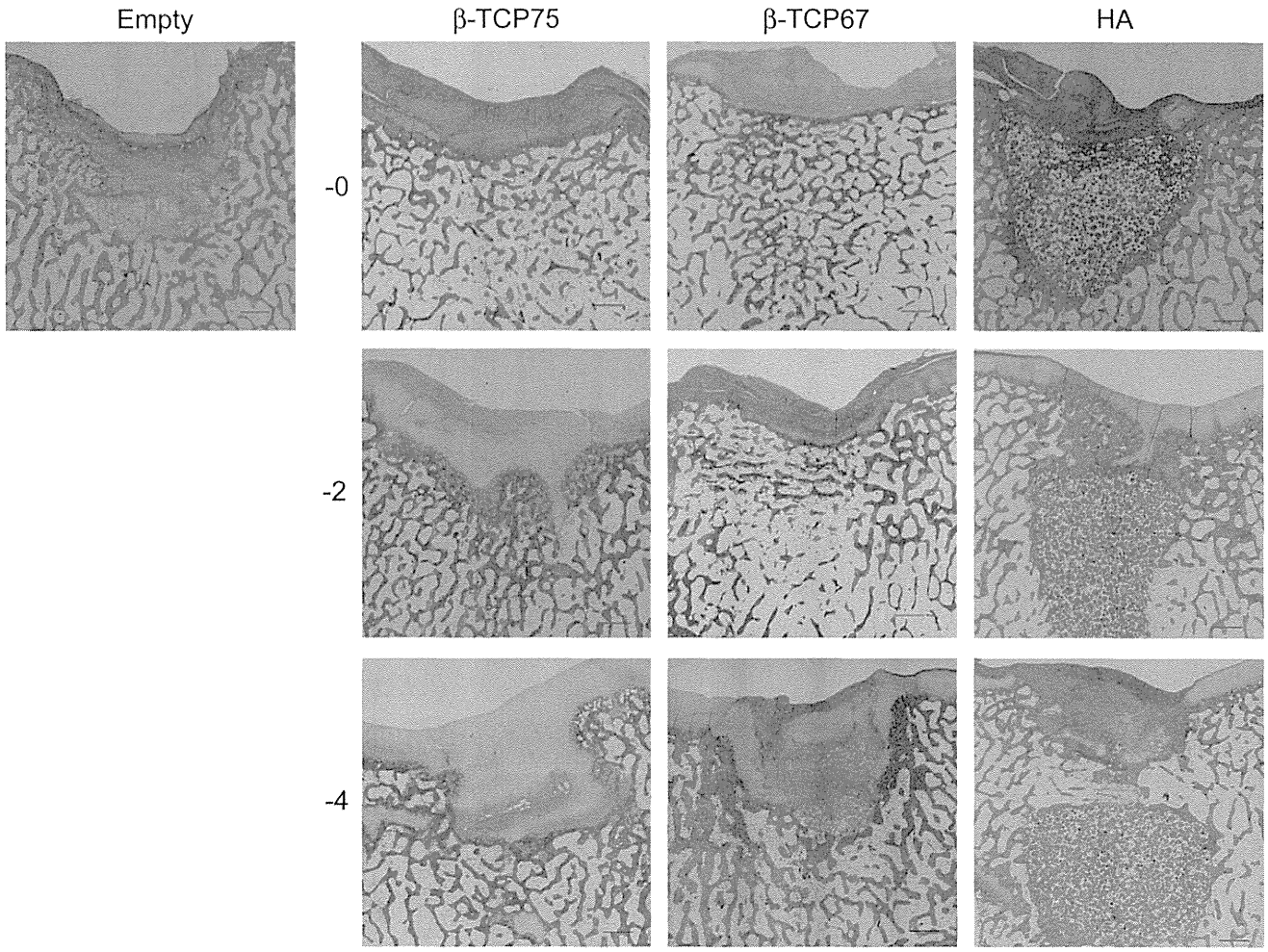

Fig. 5 Histological sections stained with hematoxylin and eosin. *Scale bars* 1,000 μm

After implanting bone substitutes, all sections showed poor staining with toluidine blue (Fig. 7).

Discussion

The most important findings of the present study were that subchondral bone defects were filled almost completely 3 months after implantation only when bone substitutes were implanted at the level of the SBP and that the reparative tissue after implanting the β-TCP bone substitutes with 75 % porosity was the most similar to the normal cancellous bone. Therefore, implanting the β-TCP bone substitutes with 75 % porosity at the level of the SBP could be recommended as a treatment method for subchondral bone repair in osteochondral defects. In addition, to our knowledge, this is the first report comparing the reparative tissue after implanting different bone substitutes at different depths in subchondral bone defects.

It has been reported that β-TCP is resorbed relatively early after implantation [20, 29, 34]. In the β-TCP75 group, CV/TV, BMD, and parameters of microarchitecture were similar to those of the normal cancellous bone 3 months after implantation. Histological sections of reparative tissue from the β-TCP75 group also resembled those of the normal cancellous bone. In addition, remaining β-TCP was undetected in the β-TCP75 group. These data suggested that most of β-TCP was resorbed and new bone was adequately formed, even in the subchondral space open to the joint cavity. Conversely, in the β-TCP67 group, CV/TV was higher than that of the normal cancellous bone, while the BMD was similar. This excessive bone formation was probably because of lower porosity (67 %) of β-TCP. Additionally, some parameters of microarchitecture in the β-TCP67 group were significantly different from those in the normal cancellous bone. Therefore, 75 % porosity was considered to be more suitable for subchondral bone repair than 67 % porosity. This difference was probably caused by the amount of β-TCP. New bone is formed along the wall of β-TCP bone substitute and simultaneously β-TCP is resorbed through hydrolysis. Therefore, inadequate β-TCP leads to inadequate bone formation, while excessive β-TCP

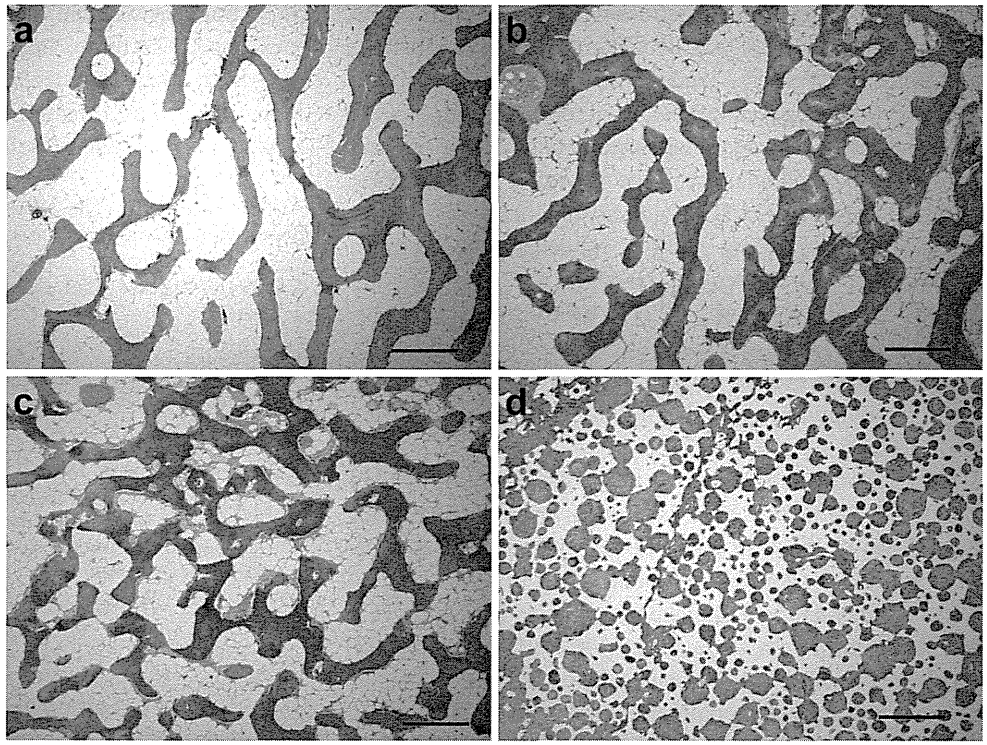

Fig. 6 Magnified views of histological sections stained with hematoxylin and eosin. **a** Normal cancellous bone. **b**, **c**, **d** Central areas of β-TCP75 group (**b**), β-TCP67 group (**c**), and HA group (**d**). *Scale bars* 500 μm

Fig. 7 A representative histological section stained with toluidine *blue*. The β-TCP with 75 % porosity was implanted at the level of the subchondral bone plate. *Scale bars* 1,000 μm

leads to excessive bone formation like in the β-TCP65 group. In the current study, the amount of β-TCP in the β-TCP75 group might be moderate for subchondral bone repair. To our knowledge, the present study is the first to show that the properties of subchondral bone are directly influenced by the porosity of bone substitutes, even if the bone substitutes are made of the same material.

On the other hand, the resorption of HA is very slow [20, 29, 34, 35]. In the current study, CV/TV and BMD of the HA group were higher than those of the normal cancellous bone probably as a result of remaining HA and newly formed bone. Additionally, most of the parameters of microarchitecture were significantly different from those of the normal cancellous bone. In addition, reparative tissue of the HA group did not histologically resemble the normal cancellous bone. According to these results, HA is not in itself a suitable material for subchondral bone repair. If a longer follow-up had been done, the result after implanting HA at 2 mm below the SBP might improve with cancellous bone formation above HA.

In all 3 implanted groups, 2-D microfocus CT analysis and histological evaluation showed that subchondral bone repair was poor when bone substitutes were implanted at 4 mm below the SBP. In the present study, subchondral bone defects were open to the joint cavity. Therefore, synovial fluid could easily flow into the defects and make osteoconduction difficult. This finding suggests that an adequate amount of osteoconductive scaffold is essential for bone formation in the presence of synovial fluid. In addition, clinicians and researchers should recognize that the depth at which bone substitutes are implanted may be a key factor in subchondral bone repair.

Regarding the treatment of osteochondral defects in this study, cartilage repair was inadequate in all three implanted

groups even when bone substitutes were implanted at the level of the SBP. This was demonstrated by poor staining with toluidine blue. The inadequate repair of cartilage was probably because of conditions being too severe for hyaline cartilage repair. However, the current study clearly showed that the quality and quantity of the reparative tissue was the best after implanting β-TCP with 75 % porosity at the level of the SBP. This finding could be expected to be useful in improving recent challenging treatments of osteochondral defects, including use of β-TCP in combination with cell-based therapy [1, 12, 27], newly developed biomaterials [3, 14], or various growth factors such as fibroblast growth factor, bone morphogenetic protein-2, and transforming growth factor-β1 [16, 18, 33].

The clinical relevance of the present study is that implanting the β-TCP bone substitutes with 75 % porosity at the level of the SBP could be recommended as a treatment method for subchondral bone repair in osteochondral defects. For example, it may be an option to implant β-TCP bone substitutes with 75 % porosity at the level of the SBP in donor sites after OAT, because donor site morbidity and its potential to lead to patellofemoral osteoarthritis are a concern [15, 22, 25, 31]. However, human clinical studies are needed to conclude this suggestion.

There were several limitations of this study. First, the biomechanical property of reparative tissue was not evaluated. However, both in microfocus CT analysis and histological evaluation, the reparative tissue of the β-TCP75 group resembled the normal cancellous bone. Therefore, it is reasonable to consider β-TCP with 75 % porosity as the most suitable bone substitute for subchondral bone repair. Second, neither microfocus CT analysis nor histological evaluation was performed sequentially. The reparative tissue in the β-TCP67 group might become similar to the normal cancellous bone over time. However, even so, the normal cancellous bone was formed more rapidly in the β-TCP75 group than that in the β-TCP67 group. Also in case of the HA group, the reparative tissue might come to resemble the normal cancellous bone after the resorption of HA. However, the resorption of HA takes a very long time [20, 29, 34, 35]. In terms of subchondral bone repair, if the bone substitute is replaced by the normal cancellous bone earlier, it would be more beneficial. Therefore, we considered β-TCP with 75 % porosity to be more suitable for subchondral bone repair than the other 2 bone substitutes.

Conclusions

Subchondral bone defects were filled almost completely 3 months after implantation only when bone substitutes were implanted at the level of the SBP. The reparative tissue after implanting the β-TCP bone substitutes with 75 % porosity was the most similar to the normal cancellous bone. Therefore, implanting the β-TCP bone substitutes with 75 % porosity at the level of the SBP could be recommended as a treatment method for subchondral bone repair in osteochondral defects.

Acknowledgments The authors would like to thank Mrs. Mari Shinkawa for her technical assistance.

Conflict of interest The authors declare that they have no conflict of interest.

References

1. Ando W, Fujie H, Moriguchi Y, Nansai R, Shimomura K, Hart DA, Yoshikawa H, Nakamura N (2012) Detection of abnormalities in the superficial zone of cartilage repaired using a tissue engineered construct derived from synovial stem cells. Eur Cell Mater 24:292–307
2. Arkill KP, Winlove CP (2008) Solute transport in the deep and calcified zones of articular cartilage. Osteoarthr Cartil 16:708–714
3. Benthien JP, Behrens P (2011) The treatment of chondral and osteochondral defects of the knee with autologous matrix-induced chondrogenesis (AMIC): method description and recent developments. Knee Surg Sports Traumatol Arthrosc 19:1316–1319
4. Delloye C, Cornu O, Druez V, Barbier O (2007) Bone allografts: what they can offer and what they cannot. J Bone Joint Surg Br 89:574–579
5. Feng YF, Wang L, Li X, Ma ZS, Zhang Y, Zhang ZY, Lei W (2012) Influence of architecture of beta-tricalcium phosphate scaffolds on biological performance in repairing segmental bone defects. PLoS One 7:e49955
6. Finkemeier CG (2002) Bone-grafting and bone-graft substitutes. J Bone Joint Surg Am 84(A):454–464
7. Goff T, Kanakaris NK, Giannoudis PV (2013) Use of bone graft substitutes in the management of tibial plateau fractures. Injury 44(Suppl 1):S86–S94
8. Goldberg VM, Stevenson S (1987) Natural history of autografts and allografts. Clin Orthop Relat Res 225:7–16
9. Gomoll AH, Madry H, Knutsen G, van Dijk N, Seil R, Brittberg M, Kon E (2010) The subchondral bone in articular cartilage repair: current problems in the surgical management. Knee Surg Sports Traumatol Arthrosc 18:434–447
10. Goto A, Murase T, Oka K, Yoshikawa H (2011) Use of the volar fixed angle plate for comminuted distal radius fractures and augmentation with a hydroxyapatite bone graft substitute. Hand Surg 16:29–37
11. Koepp HE, Schorlemmer S, Kessler S, Brenner RE, Claes L, Gunther KP, Ignatius AA (2004) Biocompatibility and osseointegration of beta-TCP: histomorphological and biomechanical studies in a weight-bearing sheep model. J Biomed Mater Res B Appl Biomater 70:209–217
12. Koga H, Engebretsen L, Brinchmann JE, Muneta T, Sekiya I (2009) Mesenchymal stem cell-based therapy for cartilage repair: a review. Knee Surg Sports Traumatol Arthrosc 17:1289–1297
13. Kurien T, Pearson RG, Scammell BE (2013) Bone graft substitutes currently available in orthopaedic practice: the evidence for their use. Bone Joint J 95(B):583–597
14. Lafantaisie-Favreau CH, Guzman-Morales J, Sun J, Chen G, Harris A, Smith TD, Carli A, Henderson J, Stanish WD, Hoemann CD (2013) Subchondral pre-solidified chitosan/blood implants elicit reproducible early osteochondral wound-repair

responses including neutrophil and stromal cell chemotaxis, bone resorption and repair, enhanced repair tissue integration and delayed matrix deposition. BMC Musculoskelet Disord 14:27
15. LaPrade RF, Botker JC (2004) Donor-site morbidity after osteochondral autograft transfer procedures. Arthroscopy 20:e69–e73
16. Lopiz-Morales Y, Abarrategi A, Ramos V, Moreno-Vicente C, Lopez-Duran L, Lopez-Lacomba JL, Marco F (2010) In vivo comparison of the effects of rhBMP-2 and rhBMP-4 in osteochondral tissue regeneration. Eur Cell Mater 20:367–378
17. Madry H, van Dijk CN, Mueller-Gerbl M (2010) The basic science of the subchondral bone. Knee Surg Sports Traumatol Arthrosc 18:419–433
18. Maehara H, Sotome S, Yoshii T, Torigoe I, Kawasaki Y, Sugata Y, Yuasa M, Hirano M, Mochizuki N, Kikuchi M, Shinomiya K, Okawa A (2010) Repair of large osteochondral defects in rabbits using porous hydroxyapatite/collagen (HAp/Col) and fibroblast growth factor-2 (FGF-2). J Orthop Res 28:677–686
19. Matsumine A, Myoui A, Kusuzaki K, Araki N, Seto M, Yoshikawa H, Uchida A (2004) Calcium hydroxyapatite ceramic implants in bone tumour surgery: a long-term follow-up study. J Bone Joint Surg Br 86:719–725
20. Mauffrey C, Seligson D, Lichte P, Pape HC, Al-Rayyan M (2011) Bone graft substitutes for articular support and metaphyseal comminution: what are the options? Injury 42(Suppl 2):S35–S39
21. Ng AM, Tan KK, Phang MY, Aziyati O, Tan GH, Isa MR, Aminuddin BS, Naseem M, Fauziah O, Ruszymah BH (2008) Differential osteogenic activity of osteoprogenitor cells on HA and TCP/HA scaffold of tissue engineered bone. J Biomed Mater Res A 85:301–312
22. Nosewicz TL, Reilingh ML, van Dijk CN, Duda GN, Schell H (2012) Weightbearing ovine osteochondral defects heal with inadequate subchondral bone plate restoration: implications regarding osteochondral autograft harvesting. Knee Surg Sports Traumatol Arthrosc 20:1923–1930
23. Oka K, Murase T, Moritomo H, Goto A, Sugamoto K, Yoshikawa H (2010) Corrective osteotomy using customized hydroxyapatite implants prepared by preoperative computer simulation. Int J Med Robot 6:186–193
24. Onodera J, Kondo E, Omizu N, Ueda D, Yagi T, Yasuda K (2013) Beta-tricalcium phosphate shows superior absorption rate and osteoconductivity compared to hydroxyapatite in open-wedge high tibial osteotomy. Knee Surg Sports Traumatol Arthrosc. doi:10.1007/s00167-013-2681-y
25. Reddy S, Pedowitz DI, Parekh SG, Sennett BJ, Okereke E (2007) The morbidity associated with osteochondral harvest from asymptomatic knees for the treatment of osteochondral lesions of the talus. Am J Sports Med 35:80–85
26. Sakamoto M, Nakasu M, Matsumoto T, Okihana H (2007) Development of superporous hydroxyapatites and their examination with a culture of primary rat osteoblasts. J Biomed Mater Res A 82:238–242
27. Shimomura K, Ando W, Tateishi K, Nansai R, Fujie H, Hart DA, Kohda H, Kita K, Kanamoto T, Mae T, Nakata K, Shino K, Yoshikawa H, Nakamura N (2010) The influence of skeletal maturity on allogenic synovial mesenchymal stem cell-based repair of cartilage in a large animal model. Biomaterials 31:8004–8011
28. Tamai N, Myoui A, Tomita T, Nakase T, Tanaka J, Ochi T, Yoshikawa H (2002) Novel hydroxyapatite ceramics with an interconnective porous structure exhibit superior osteoconduction in vivo. J Biomed Mater Res 59:110–117
29. Tamai N, Myoui A, Kudawara I, Ueda T, Yoshikawa H (2010) Novel fully interconnected porous hydroxyapatite ceramic in surgical treatment of benign bone tumor. J Orthop Sci 15:560–568
30. Tomford WW (1995) Transmission of disease through transplantation of musculoskeletal allografts. J Bone Joint Surg Am 77:1742–1754
31. Valderrabano V, Leumann A, Rasch H, Egelhof T, Hintermann B, Pagenstert G (2009) Knee-to-ankle mosaicplasty for the treatment of osteochondral lesions of the ankle joint. Am J Sports Med 37(Suppl 1):105S–111S
32. Van Hoff C, Samora JB, Griesser MJ, Crist MK, Scharschmidt TJ, Mayerson JL (2012) Effectiveness of ultraporous beta-tricalcium phosphate (vitoss) as bone graft substitute for cavitary defects in benign and low-grade malignant bone tumors. Am J Orthop 41:20–23
33. Wang W, Li B, Yang J, Xin L, Li Y, Yin H, Qi Y, Jiang Y, Ouyang H, Gao C (2010) The restoration of full-thickness cartilage defects with BMSCs and TGF-beta 1 loaded PLGA/fibrin gel constructs. Biomaterials 31:8964–8973
34. Yamasaki N, Hirao M, Nanno K, Sugiyasu K, Tamai N, Hashimoto N, Yoshikawa H, Myoui A (2009) A comparative assessment of synthetic ceramic bone substitutes with different composition and microstructure in rabbit femoral condyle model. J Biomed Mater Res B Appl Biomater 91:788–798
35. Yoshikawa H, Tamai N, Murase T, Myoui A (2009) Interconnected porous hydroxyapatite ceramics for bone tissue engineering. J R Soc Interface 6(Suppl 3):S341–S348

Freely available online OPEN ACCESS

BJR

■ RESEARCH

Cyclic compressive loading on 3D tissue of human synovial fibroblasts upregulates prostaglandin E2 via COX-2 production without IL-1β and TNF-α

K. Shimomura,
T. Kanamoto,
K. Kita,
Y. Akamine,
N. Nakamura,
T. Mae,
H. Yoshikawa,
K. Nakata

From Osaka University Graduate School of Medicine, Osaka, Japan

■ K. Shimomura, MD, PhD, Orthopaedic Surgeon
■ T. Kanamoto, MD, PhD, Orthopaedic Surgeon
■ K. Kita, MD, PhD, Orthopaedic Surgeon
■ Y. Akamine, DMD, PhD, Dental Doctor
■ T. Mae, MD, PhD, Orthopaedic Surgeon
■ H. Yoshikawa, MD, PhD, Orthopaedic Surgeon, Professor Osaka University Graduate School of Medicine, Department of Orthopaedics, 2-2 Yamadaoka, Suita City, Osaka 565-0871, Japan.

■ N. Nakamura, MD, PhD, Orthopaedic Surgeon, Professor Osaka Health Science University, Department of Rehabilitation Science, 1-9-27 Tenma, Kita-ku, Osaka City, Osaka 530-0043, Japan.

■ K. Nakata, MD, PhD, Orthopaedic Surgeon, Professor Osaka University Graduate School of Medicine, Department of Health and Sport Sciences, 1-17 Machikaneyamacho, Toyonaka, Osaka 560-0043, Japan.

Correspondence should be sent to Prof K. Nakata; e-mail: ken-nakata@umin.ac.jp

10.1302/2046-3758.39.2000287
$2.00

Bone Joint Res 2014;9:280–8.
Received 13 February 2014;
Accepted 16 April 2014

Objective

Excessive mechanical stress on synovial joints causes osteoarthritis (OA) and results in the production of prostaglandin E2 (PGE2), a key molecule in arthritis, by synovial fibroblasts. However, the relationship between arthritis-related molecules and mechanical stress is still unclear. The purpose of this study was to examine the synovial fibroblast response to cyclic mechanical stress using an *in vitro* osteoarthritis model.

Method

Human synovial fibroblasts were cultured on collagen scaffolds to produce three-dimensional constructs. A cyclic compressive loading of 40 kPa at 0.5 Hz was applied to the constructs, with or without the administration of a cyclooxygenase-2 (COX-2) selective inhibitor or dexamethasone, and then the concentrations of PGE2, interleukin-1β (IL-1β), tumour necrosis factor-α (TNF-α), IL-6, IL-8 and COX-2 were measured.

Results

The concentrations of PGE2, IL-6 and IL-8 in the loaded samples were significantly higher than those of unloaded samples; however, the concentrations of IL-1β and TNF-α were the same as the unloaded samples. After the administration of a COX-2 selective inhibitor, the increased concentration of PGE2 by cyclic compressive loading was impeded, but the concentrations of IL-6 and IL-8 remained high. With dexamethasone, upregulation of PGE2, IL-6 and IL-8 was suppressed.

Conclusion

These results could be useful in revealing the molecular mechanism of mechanical stress *in vivo* for a better understanding of the pathology and therapy of OA.

Cite this article: *Bone Joint Res* 2014;3:280–8.

Keywords: Mechanical stress, Osteoarthritis, 3-D culture, Synovial fibroblast, Prostaglandin E2

Article focus

- Analysis of molecular mechanism of osteoarthritis (OA) development
- Analysis of mechanotransduction in OA development
- Function of synovial fibroblast in OA development

Key messages

- Cyclic compressive loading on a 3D cultured construct of human fibroblasts upregulated PGE2 via COX-2 production
- Cyclic compressive loading upregulated interleukin-6 (IL-6) and IL-8 proteins
- The expression of these molecules was upregulated without IL-1β and/or tumour necrosis factor (TNF)-α stimulation

Strengths and limitations

- Strengths - our 3D culture system is close to intra-articular environment
- Our system could be useful in revealing the molecular mechanism of mechanical stress
- Limitation - the intracellular signal transductions of PGE2, IL-6 and IL-8 (mechanotransduction) have not been clarified

Introduction

Osteoarthritis (OA) is a common disease that causes joint pain, deformity and functional disability, and is increasingly prevalent in hundreds of millions of people worldwide.[1] Congenital disorders, obesity, labour, sports, malalignment and joint instability may

initiate processes leading to loss of cartilage. In addition, repeated excessive mechanical stress on the synovial joint, which is composed of cartilage and synovium, is considered to be a key factor in OA development. However, the molecular relationship between mechanical stress and OA development is still unclear.

OA involves a variable degree of synovitis, and these inflammations cause many symptoms including joint swelling and effusion in clinical situations.[2-6] Synovial fibroblasts and macrophages, as well as chondrocytes, play an important role in OA development through synovitis, and synovial macrophages are considered to produce pro-inflammatory cytokines, such as interleukin-1β (IL-1β) and tumour necrosis factor-α (TNF-α).[6-10] These cytokines stimulate synovial fibroblasts and chondrocytes to produce other cytokines, such as IL-6 and IL-8, and several enzymes, such as matrix metalloproteinases (MMPs) and aggrecanases (ADAMTSs). These enzymes sever type II collagen and proteoglycan, the principal components of the extracellular matrix of articular cartilage.[11-15] In addition, prostaglandin E2 (PGE2) plays a significant role in OA by causing pain, inflammation, and cartilage degradation.[16-18] Although PGE2 is known to be produced by synovial fibroblasts or chondrocytes in response to IL-1β and/or TNF-α, which is produced by synovial macrophages,[19-21] the molecular mechanism of PGE2 production triggered by mechanical stress is still unclear.

We have developed a novel three-dimensional (3D) culture system using cyclic mechanical stress on synovial cells or chondrocytes for revealing the molecular mechanism of OA development resulting from mechanical stress. In particular, we have focused on synovial cells, which play an important role in OA development as mentioned above. In our previous study, we have shown that cyclic mechanical stress on 3D cultured constructs of human synovial fibroblasts upregulated mRNA levels of MMP1, MMP2, MMP3, MMP9, MMP13, ADAMTS4, and ADAMTS5 genes in a load-dependent manner[22-23] however, the induction of PGE2 as a result of mechanical stress has not been investigated. In the PGE2 synthesis pathway, cyclooxygenase-2 (COX-2) and microsomal prostaglandin E synthase-1 (mPGES-1) are key enzymes that metabolise arachidonic acid to PGE2.[24,25] Nonsteroidal anti-inflammatory drugs (NSAIDs) and steroids, which downregulate PGE2 synthesis through inhibition of COX-2 activity, have been widely used in the treatment of OA.[19]

The purpose of this study was to examine the expression of PGE2 and the related cytokine expressions of IL-1β, TNF-α, IL-6 and IL-8 by cyclic compressive loading on 3D cultured constructs of human synovial fibroblasts and to clarify the effects of NSAIDs and steroids using our *in vitro* OA model.

Materials and Methods

Cell culture of primary human synovial fibroblasts. Human synovial membranes were obtained aseptically from eight patients aged from 17 to 34 years (three male, five female) who underwent arthroscopic knee surgery in accordance with a protocol approved by the Osaka University Institutional Ethical Committee. We followed the Helsinki Declaration and obtained written informed consent from all the patients involved in this study. The cell isolation protocol was essentially the same as the protocol used previously for the isolation of human synovial fibroblasts.[22,26] In brief, synovial membrane specimens were rinsed with phosphate-buffered saline (PBS), minced meticulously and digested with 0.4% collagenase XI (Sigma-Aldrich, St. Louis, Missouri) for two hours at 37°C. After neutralisation of the collagenase with a growth medium containing high-glucose Dulbecco's Modified Eagle's Medium (HG-DMEM, Wako, Osaka, Japan) supplemented with 10% fetal bovine serum (FBS; HyClone, Logan, Utah) and 1% penicillin/streptomycin (Gibco BRL, Life Technologies Inc., Carlsbad, California), the cells were collected by centrifugation, washed with PBS, resuspended in a growth medium, and plated in culture dishes. For expansion, cells were cultured in the growth medium at 37°C in a humidified atmosphere of 5% CO_2. The medium was replaced once a week. After ten to 14 days of primary culture, when the cells reached near confluence, they were washed twice with PBS, harvested by treatment with trypsin-EDTA (0.25% trypsin and 1 mM EDTA; Gibco BRL, Life Technologies Inc.), and replated at 1:3 dilution for the first subculture. Cell passages were continued in the same manner with 1:3 dilution when cultures reached near confluence. Cells at passages 3 to 7 were used in the present study.

Cell seeding on collagen scaffold and production of the 3D engineered construct. The primary cultured cells were harvested and seeded on collagen scaffolds to produce 3D constructs as previously described.[22,23] In brief, the cultured cells (5×10^5/scaffold) were suspended in a growth medium and then mixed with an equal volume of 1% Atelocollagen gel (Koken, Tokyo, Japan) on ice to produce a cell suspension in 0.5% collagen solution. The cell suspension was incorporated into collagen scaffolds (Atelocollagen Sponge Mighty, Koken, Tokyo, Japan; 5 mm diameter, 3 mm thick) by centrifugation at 500 × g for five minutes. The collagen scaffold which we used has an interconnected pore size of 30 nm to 200 nm. The scaffolds were fabricated via the process of freeze-drying of 10% collagen gel and cross-linking to reinforce the mechanical property. This is similar to those of articular cartilage. The cell–scaffold constructs were then incubated at 37°C for gelation to produce 3D cell–scaffold constructs (Fig. 1a). The cells in the 3D construct were evenly embedded in the collagen scaffold, with no cell leakage and collagen breakage after cell seeding, as we have previously shown with histological evaluation.[22] The constructs were maintained in a growth medium of HG-DMEM, with 10% FBS in free-swelling conditions at 37°C and in 5% CO_2 for three days prior to the application of cyclic load stimulation.

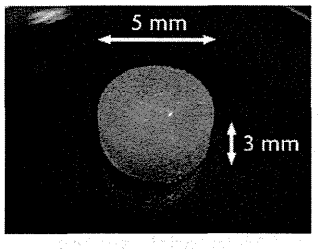

Fig. 1a

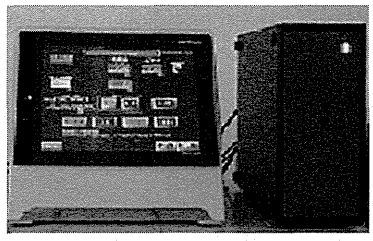

Fig. 1b

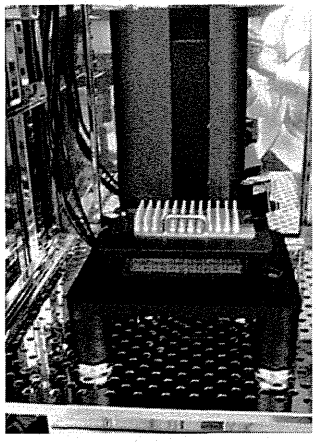

Fig. 1c

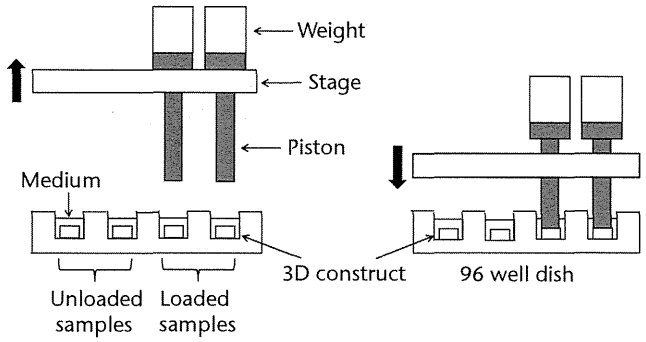

Fig. 1d

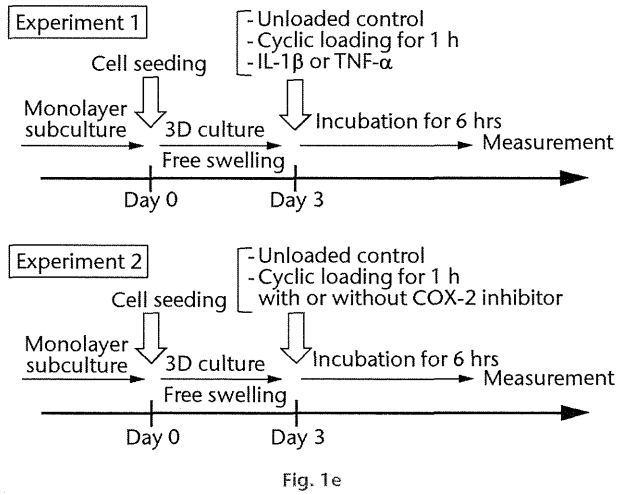

Fig. 1e

Figure 1a – 3D cell–scaffold constructs made using collagen scaffolds (AtelloCell, MIGHTY); b) monitor and controller; c) Cyclic load stimulater (CLS-5J-Z, Technoview, Osaka, Japan) in the incubator; d) Schematic representation of the cyclic load stimulator, cyclic-loaded samples, and unloaded samples; e) Experimental protocol for cyclic compressive loading on 3D constructs.

Cyclic compressive loading on 3D constructs. Cyclic unconfined compressive loading was applied to the 3D constructs using a custom-designed apparatus, a cyclic load bioreactor (CLS-5J-Z, Technoview, Osaka, Japan), as previously described (Figs 1b to 1d).[23] In brief, the loading experiments were performed with metal platens and plastic culture dishes in HG-DMEM and 10% FBS in a humidified incubator maintained at a temperature of 37°C in 5% CO_2. In all of these experiments, a cyclic compressive load of 40 kPa was applied to the constructs for one hour at the rate of 0.5 Hz, in accordance with the protocol used previously, in order to detect the expression of PGE2, IL-1β, IL-6, IL-8 and TNF-α more easily.[22,23] As mentioned above, a cyclic compressive load of 40 kPa was chosen, which yielded a 10% compression strain (approximately), because it maximally induced the mRNA expression of MMP1, MMP3, MMP9, MMP13 genes compared with the lower compressive loading of 0 kPa or 20 kPa in our previous study.[22] In addition, we measured the expression of PGE2 and the related cytokine expressions six hours after cyclic loading according to our previous study, in which the expression of MMPs maximally upregulated at this time.[22]

Experimental design. The experimental design is illustrated in Fig. 1e. On day 0, the primary cultured human synovial fibroblasts were harvested, seeded on collagen scaffolds, and maintained in growth media for three days in free-swelling conditions. For the first experiment, on day three, cyclic compressive loading was applied to the 3D constructs for one hour. 3D constructs without

loading were considered to be the control. After six hours, culture supernatant was collected, and the concentrations of PGE2, IL-1β, TNF-α, IL-6 and IL-8 were measured with the homogeneous time-resolved fluorescence (HTRF) method (described below in detail). In addition, the mRNA expression of COX-2 and mPGES-1 genes were quantitatively measured using a real-time polymerase chain reaction (PCR). In contrast to the cyclic loading, 10 ng/ml of IL-1β (R&D Systems, Minneapolis, Minnesota) or 100 ng/ml of TNF-α (R&D Systems) was administered to the unloaded 3D constructs on day three. A total of six hours after the administration of these cytokines, the concentration of PGE2 in culture supernatant was measured using HTRF. For the second experiment, cyclic compressive loading was applied to the 3D constructs with or without two types of COX-2 inhibitors: COX-2 selective inhibitor (celecoxib, provided by Pfizer Japan Inc., Tokyo, Japan) or dexamethasone (Sigma-Aldrich). These drugs were administered just before cyclic compressive loading was applied. Six hours after cyclic loading, the concentrations of PGE2, IL-6 and IL-8 in culture supernatant were measured using HTRF. In addition, the mRNA expression of the COX-2 gene was quantitatively estimated by real-time PCR.

Quantitative protein analysis of culture supernatant using HTRF. For each culture supernatant sample, an enzyme immunoassay was performed to measure the concentrations of PGE2, IL-1β, TNF-α, IL-6 and IL-8 using HTRF human PGE2, IL-1β, TNF-α, IL-6 and IL-8 assay kits (CIS Bio International, Saclay, France).

Quantitative mRNA expression analysis of COX-2 and mPGES-1 genes. Total RNAs from the 3D constructs were extracted using a RNeasy mini kit (Qiagen, Valencia, California). Complementary DNAs (cDNAs) were obtained by the use of a reverse transcription (RT) of 200 μg of total RNA through the use of a reverse transcription system (Promega, San Luis Obispo, California) with random primers. For the quantification of gene expression, PCR amplification was performed with SYBR Premix ExTaq (Takara Bio, Shiga, Japan) on a LightCycler 1.5 real-time PCR system (Roche, Indianapolis, Indiana). RNA expression levels were normalised to that of GAPDH. The primers used were as follows: human GAPDH (forward): TCT CTG CTC CTC CTG TTC GAC, (reverse): GTT GAC TCC GAC CTT CAC CTT C, human COX-2 (forward): AGG GTT GCT GGT GGT AGG AA, (reverse): GGT CAA TGG AAG CCT GTG ATA CT, human mPGES-1 (forward): CCT GGG CTT CGT CTA CTC CTT, (reverse): AGT GCA TCC AGG CGA CAA A.

Statistical analysis. Every experiment was performed more than three times using independent donors. Statistical analysis was performed with analysis of variance (ANOVA) followed by *post hoc* testing (> 2 groups). The comparison of other parameters was analysed with a Mann–Whitney U test (two groups). The results are presented as mean and SD. The data were analysed with JMP 9 (SAS Institute, Cary, North Carolina) and significance was set at $p < 0.05$.

Results

The expressions of PGE2 and related molecules by cyclic compressive loading. The concentrations of PGE2, IL-6 and IL-8 in a culture supernatant of loaded samples were significantly higher compared with that of unloaded samples (PGE2, 0.33 ng/ml (SD 0.055) *vs* 2.07 ng/ml (SD 0.65), $p < 0.01$ (Fig. 2a); IL-6, 0.71 ng/ml (SD 0.42) *vs* 6.89 (SD 0.25), $p < 0.01$ (Fig. 2b); and IL-8, 0.77 ng/ml (SD 0.39) *vs* 8.76 ng/ml (SD 0.69), $p < 0.01$ (Fig. 2c)). However, the concentrations of IL-1β and TNF-α were unchanged between loaded and unloaded samples (IL-1β, 4.8 pg/ml (SD 8.2) *vs* 7.4 pg/ml (SD 8.4), $p = 0.74$ (Fig. 2d) and TNF-α, 9.6 pg/ml (SD 8.8) *vs* 7.6 pg/ml (SD 8.3), $p = 0.75$ (Fig. 2e)). The administration of IL-1β or TNF-α also significantly induced PGE2 production compared with the non-administered control (IL-1β, 0.33 ng/ml (SD 0.055) *vs* 2.25 ng/ml (SD 0.65), $p < 0.01$ and TNF-α, 0.33 ng/ml (SD 0.055) *vs* 1.84 ng/ml (SD 0.63), $p < 0.01$ (Fig. 2a)). The mRNA levels of COX-2 and mPGES-1 genes of loaded samples were significantly higher compared with that of unloaded samples (COX-2, 1 *vs* 6.97 (SD 3.66), $p < 0.01$ (Fig. 2f); mPGES-1, 1 *vs* 5.03 (SD 2.94), $p < 0.01$ (Fig. 2g)).

The effects of a COX-2 selective inhibitor on mechanically induced PGE2, IL-6 and IL-8 proteins and COX-2 gene expressions. The increased concentration of PGE2 by cyclic compressive loading was impeded in a dose-dependent manner after administration of a COX-2 selective inhibitor (Fig. 3a). More than 100 nM of a COX-2 selective inhibitor significantly abolished the upregulation of PGE2 by cyclic compressive loading ($p < 0.01$). However, the increased concentration of IL-6 and IL-8 by cyclic compressive loading remained high, and the inhibitory effects of the COX-2 selective inhibitor were not observed (Figs 3b and 3c). The upregulation of COX-2 mRNA levels by cyclic compressive loading was not suppressed by a COX-2 selective inhibitor (Fig. 3d).

The effects of dexamethasone on mechanically induced PGE2, IL-6 and IL-8 proteins and COX-2 gene expressions. The increased concentration of PGE2 by cyclic compressive loading was suppressed in a dose-dependent manner after administration of dexamethasone (Fig. 4a). More than 100 nM of dexamethasone significantly abolished the upregulation of PGE2 by cyclic compressive loading ($p < 0.01$). Similarly, the increased concentration of IL-6 and IL-8 was also suppressed in a dose-dependent manner (Figs 4b and 4c). More than 100 nM of dexamethasone significantly abolished the upregulation of IL-6 or IL-8 by cyclic compressive loading ($p < 0.01$). The upregulation of COX-2 mRNA levels by cyclic compressive loading was suppressed in a dose-dependent manner after the administration of dexamethasone (Fig. 4d). More than 10 nM of dexamethasone significantly abolished the upregulation of COX-2 mRNA levels by cyclic compressive loading ($p < 0.01$).

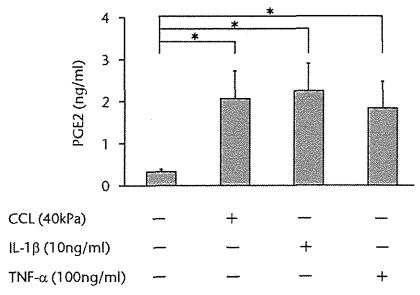

Fig. 2a

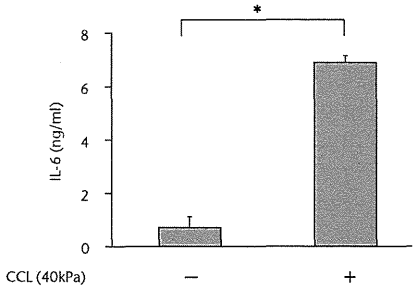

Fig. 2b

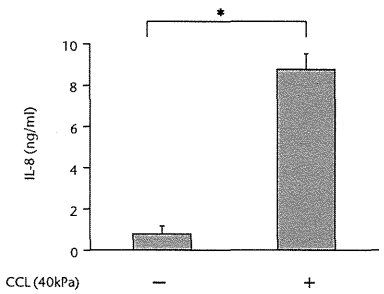

Fig. 2c

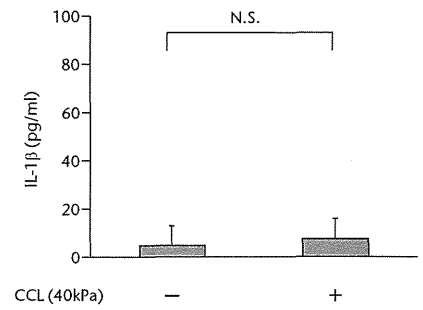

Fig. 2d

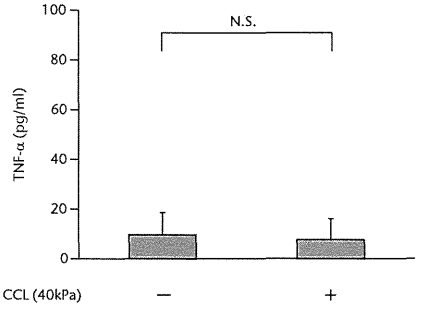

Fig. 2e

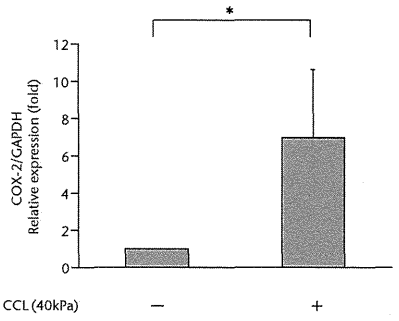

Fig. 2f

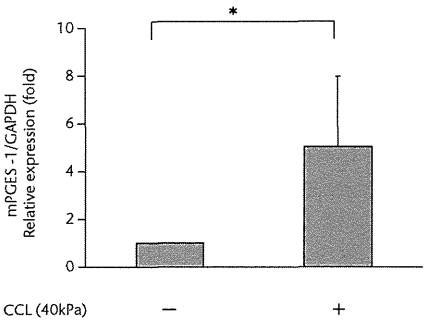

Fig. 2g

Graphs showing the expressions of PGE2 and related molecules by cyclic compressive loading. a) PGE2 was significantly upregulated by cyclic compressive loading, interleukin- (IL-)1β, or tumour necrosis factor- (TNF)-α (n = 7). b) IL-6 (n = 6) and c) IL-8 (n = 6) were significantly upregulated by cyclic compressive loading. d) IL-1β (n = 6) and e) TNF-α (n = 6) were not upregulated by cyclic compressive loading. f) COX-2 (n = 6) and g) mPGES-1 (n = 5) mRNA levels were significantly upregulated by cyclic compressive loading (CCL;cyclic compressive loading)*p < 0.01.

Discussion

Mechanical stress is believed to be important for every cell in our body, particularly intra-articular tissues such as bone, cartilage, meniscus, and synovium, for the maintenance and regeneration of tissues and organs. Many studies have demonstrated that mechanical stress to chondrocytes, cartilage explants, or mesenchymal stem cells promoted bone and cartilage development.[27-30] However, mechanical stress causes joint diseases, and excessive mechanical stress may lead to the development of OA. PGE2 is well known as a pathogenic molecule related to OA development, in addition to MMPs, ADAMTS, and inflammatory cytokines.[31] To investigate the molecular mechanisms of PGE2 and related inflammatory cytokines by mechanical stress, we used the 3D culture system using cyclic compressive loading, which can mimic the intra-articular environment through the adjustment of magnitudes, durations, and frequencies of loads. The loading condition of this study represents that cyclic loading for one hour at a rate of 0.5 Hz is nearly equal to the walking pace. We have chosen 40 kPa, which yielded approximately 10% compression strain, because it maximally induced mRNA expression of MMP1, MMP3, MMP9 and MMP13 genes compared with the lower compressive loading of 0 kPa or 20 kPa in our previous study.[22] In addition, there have been no obvious data of biomechanics in synovium as far as we know, while > 10% compression strain to cartilage was shown to inhibit proteoglycan and protein synthesis in a dose-dependent manner in bovine calf cartilage.[32-34] Therefore, this loading condition may be considered excessive loading over the physiological conditions. Also, the

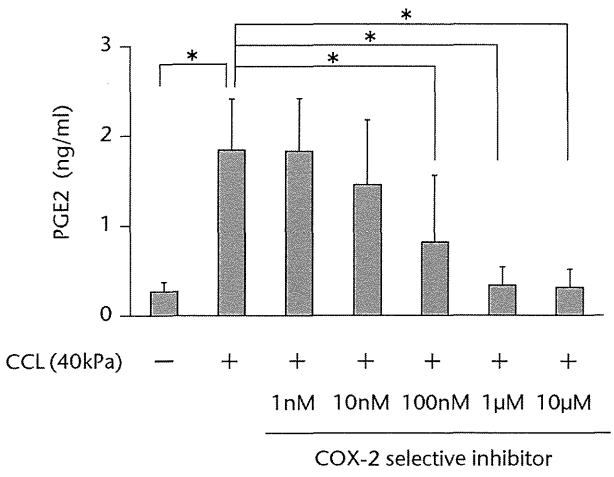

Fig. 3a

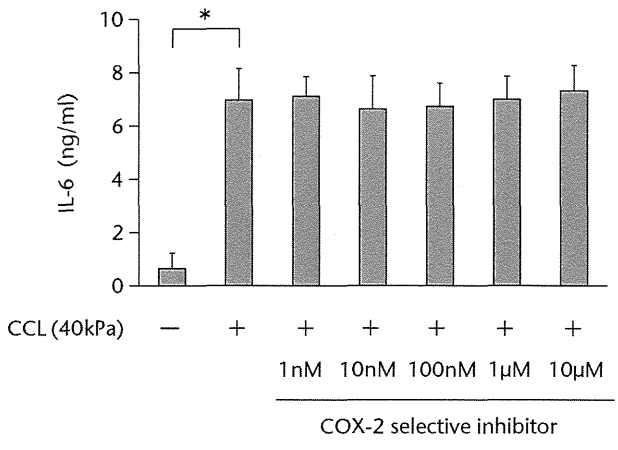

Fig. 3b

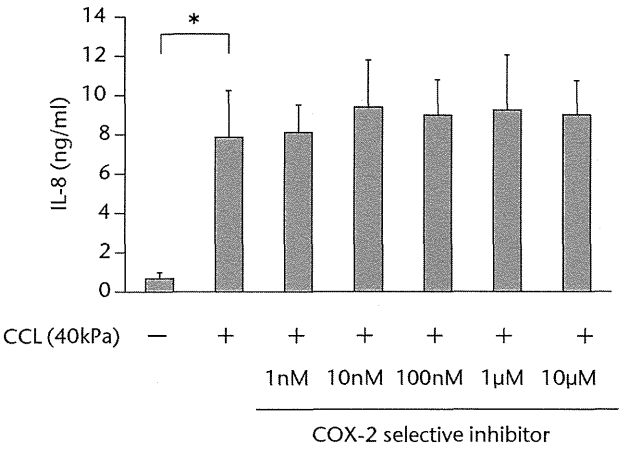

Fig. 3c

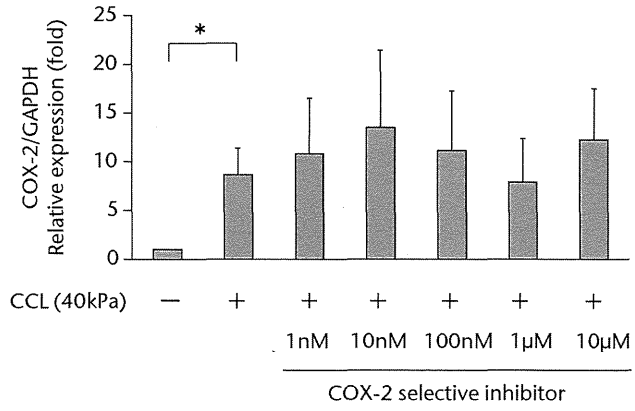

Fig. 3d

a) The increased concentration of PGE2 by cyclic compressive loading was impeded in a dose-dependent manner (n = 8). b) The increased concentrations of IL-6 (n = 7) and c) IL-8 (n = 5) by cyclic compressive loading remained high. d) The upregulation of COX-2 mRNA levels by cyclic compressive loading was not suppressed by a COX-2 selective inhibitor (n = 5). *p < 0.01

loading was applied with uni-axial unconfined compression, and this condition could also mimic the intra-articular environment, in which both compressive and tensile stresses are applied to the synovium.[23,35,36] Moreover, a 3D culture system is better to evaluate a biological reaction, because 3D culture is close to the physical environment and there are sometimes differences detected between 2D and 3D cultures.[37-41]

In this study, we directly demonstrated that cyclic compressive loading on a 3D-cultured construct of human synovial fibroblasts upregulated PGE2, IL-6 and IL-8 proteins. We also showed that the gene expression of COX-2 and mPGES-1, which are the key enzymes that metabolise arachidonic acid to PGE2, was upregulated by cyclic compressive loading (Fig. 5). In addition, the upregulation of PGE2 by cyclic compressive loading was suppressed by the administrations of a COX-2 selective inhibitor or dexamethasone in a dose-dependent manner. As a pharmacological effect, COX-2 selective inhibitors inhibit the activity of COX-2, whereas dexamethasone inhibits the synthesis of COX-2.[42-45] In this study, a COX-2 selective inhibitor suppressed PGE2 production in a dose-dependent manner without changing the COX-2 mRNA level, whereas dexamethasone suppressed PGE2 production by suppressing the COX-2 gene expression. These results reflect well with the pharmacology of PGE2 inhibition by NSAIDs and steroids in OA. Interestingly, a COX-2 selective inhibitor did not suppress IL-6 and IL-8 production, whereas dexamethasone suppressed these cytokines in a dose-dependent manner. The different effects of these chemicals on IL-6 and IL-8 may account for the distinct functions in clinical usage.

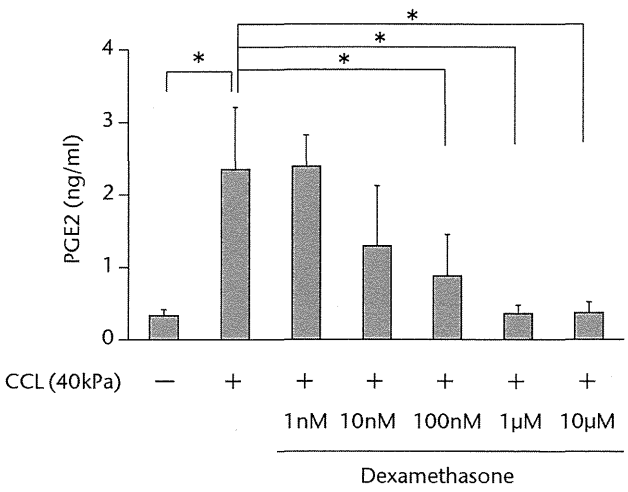

Fig. 4a

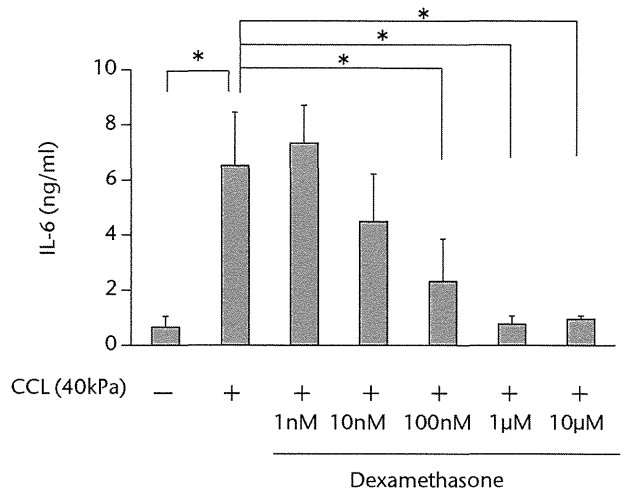

Fig. 4b

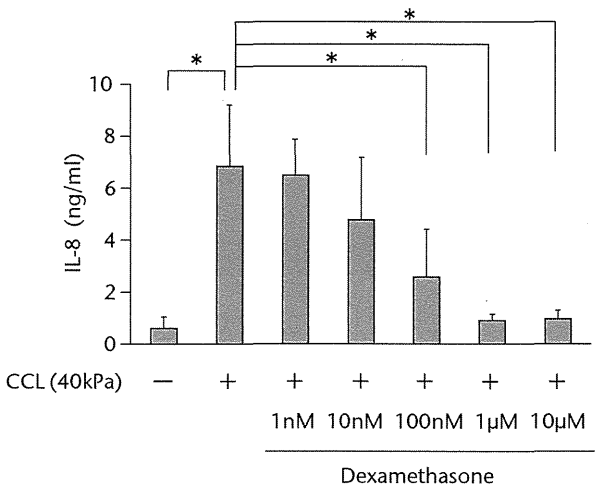

Fig. 4c

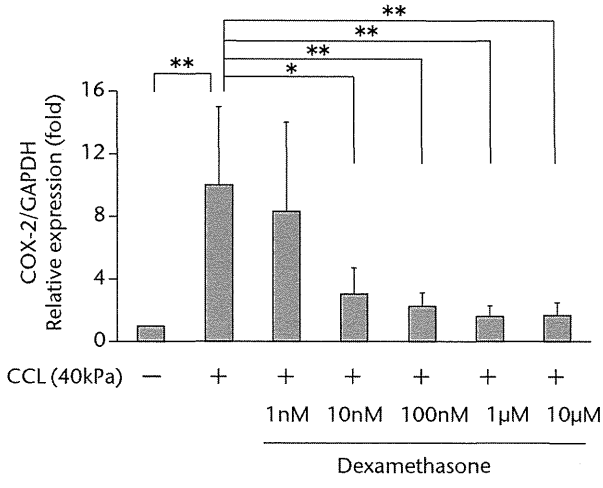

Fig. 4d

Graphs showing the effects of dexamethasone on mechanically induced PGE2, interleukin- (IL-)6, and IL-8 proteins and COX-2 gene expressions. The increased concentrations of a) PGE2 (n = 5), b) IL-6 (n = 5), and c) IL-8 (n = 5) by cyclic compressive loading were suppressed in a dose-dependent manner. d) The upregulation of COX-2 mRNA levels by cyclic compressive loading was also suppressed in a dose-dependent manner (n = 5). *p < 0.05 **p < 0.01

These functions are still unclear and further studies are required.

Synovial fibroblasts did not produce IL-1β and TNF-α by cyclic compressive loading in this study, as reported previously.[6-10] To our surprise, however, synovial fibroblasts produced PGE2, IL-6 and IL-8 without the stimulation of IL-1β and TNF-α, which are produced by synovial macrophages. Undoubtedly, IL-1β and TNF-α, produced by synovial macrophages, are considered to be key factors for OA development through the production of PGE2, MMPs, and ADAMTSs by synovial fibroblasts and chondrocytes.[2,5,6,15,20,46-50] On the other hand, it has been unclear what triggers the activation of synovial macrophages. In this study, PGE2 was significantly upregulated by cyclic compressive loading without IL-1β and TNF-α stimulation. Also, we have previously demonstrated that cyclic mechanical stress on synovial fibroblasts upregulated mRNA levels of MMP1, MMP2, MMP3, MMP9, MMP13, ADAMTS4 and ADAMTS5 genes in a load-dependent manner through the same experiment.[22,23] Taken together, the upregulation of the key molecules of OA development including PGE2, MMPs, and ADAMTSs was induced by mechanical stress without the upregulation of IL-1β and/or TNF-α. In our opinion, therefore, excessive mechanical stress may 'switch on' these gene expressions as the trigger of OA development without IL-1β and/or TNF-α stimulation. (Fig. 5) This notion may coincide with some previous studies using animals and clinical samples, which showed that IL-1β and/or TNF-α were not necessary in OA development.[51-53]

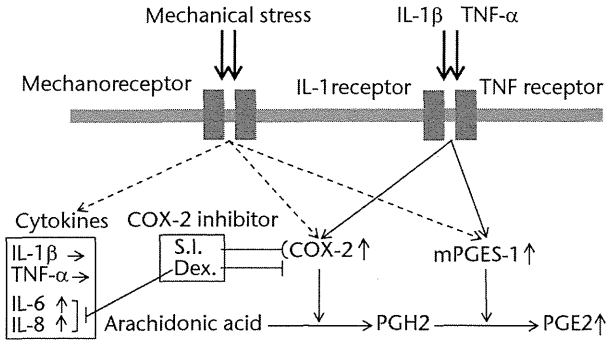

Fig. 5

Schematic representation of the relationship between mechanical stress and the expression of PGE2 and related molecules. Cyclic compressive loading on a 3D cultured construct of human fibroblasts upregulated PGE2, interleukin- (IL-)6 and IL-8 proteins and COX-2, mPGES-1 mRNA levels without IL-1β and tumour necrosis factor- (TNF)-α stimulation. These results indicate that PGE2 upregulation may not be induced via an IL-1β and/or a TNF-α signaling pathway but via other signaling pathways (S.I.; selective inhibitor, Dex; dexamethasone).

IL-1β-deficient mice showed development of OA.[51] Moreover, the recent clinical study showed that IL-1β and TNF-α in the synovial fluid of patients with OA were not significantly higher than that in the control group.[52,53] Therefore, it can be explained that mechanical stress alone is possible to initiate OA development without the stimulation of proinflammatory cytokines.

In a potential limitation of the present study, we did not evaluate other intra-articular cells, such as chondrocytes and meniscal cells. These cells also play an important role in the development of OA. Also, the intracellular signal transductions of PGE2, IL-6 and IL-8 (mechanotransduction) have not been described in detail. In a recent study, mechanotransductions were reported to be related to the Smad pathway,[54,55] mitogen-activated protein kinase pathway,[56-58] or Wnt signaling pathway.[59-61] Our 3D culture system may be useful for the explanation of intracellular mechanotransduction.

In conclusion, cyclic compressive loading on a 3D cultured construct of human fibroblasts upregulated PGE2, IL-6 and IL-8 proteins and COX-2 and mPGES-1 mRNA levels, without IL-1β and TNF-α stimulation. Further investigation may be useful in revealing the molecular mechanism of mechanical stress *in vivo* for a better understanding of the pathology and therapy of OA.

References

1. **Harris ED Jr.** The bone and joint decade: a catalyst for progress. *Arthritis Rheum* 2001;44:1969–1970.
2. **Pelletier JP, Martel-Pelletier J, Abramson SB.** Osteoarthritis, an inflammatory disease: potential implication for the selection of new therapeutic targets. *Arthritis Rheum* 2001;44:1237–1247.
3. **Farahat MN, Yanni G, Poston R, Panayi GS.** Cytokine expression in synovial membranes of patients with rheumatoid arthritis and osteoarthritis. *Ann Rheum Dis* 1993;52:870–875.
4. **Smith MD, Triantafillou S, Parker A, Youssef PP, Coleman M.** Synovial membrane inflammation and cytokine production in patients with early osteoarthritis. *J Rheumatol* 1997;24:365–371.
5. **Benito MJ, Veale DJ, FitzGerald O, van den Berg WB, Bresnihan B.** Synovial tissue inflammation in early and late osteoarthritis. *Ann Rheum Dis* 2005;64:1263–1267.
6. **Bondeson J, Blom AB, Wainwright S, et al.** The role of synovial macrophages and macrophage-produced mediators in driving inflammatory and destructive responses in osteoarthritis. *Arthritis Rheum* 2010;62:647–657.
7. **Bartok B, Firestein GS.** Fibroblast-like synoviocytes: key effector cells in rheumatoid arthritis. *Immunol Rev* 2010;233:233–255.
8. **Huber LC, Distler O, Tarner I, et al.** Synovial fibroblasts: key players in rheumatoid arthritis. *Rheumatology (Oxford)* 2006;45:669–675.
9. **Abeles AM, Pillinger MH.** The role of the synovial fibroblast in rheumatoid arthritis: cartilage destruction and the regulation of matrix metalloproteinases. *Bull NYU Hosp Jt Dis* 2006;64:20–24.
10. **Smith TJ.** Insights into the role of fibroblasts in human autoimmune diseases. *Clin Exp Immunol* 2005;141:388–397.
11. **Little CB, Meeker CT, Golub SB, et al.** Blocking aggrecanase cleavage in the aggrecan interglobular domain abrogates cartilage erosion and promotes cartilage repair. *J Clin Invest* 2007;117:1627–1636.
12. **Glasson SS, Askew R, Sheppard B, et al.** Deletion of active ADAMTS5 prevents cartilage degradation in a murine model of osteoarthritis. *Nature* 2005;434:644–648.
13. **Stanton H, Rogerson FM, East CJ, et al.** ADAMTS5 is the major aggrecanase in mouse cartilage in vivo and in vitro. *Nature* 2005;434:648–652.
14. **Kawaguchi H.** Regulation of osteoarthritis development by Wnt-beta-catenin signaling through the endochondral ossification process. *J Bone Miner Res* 2009;24:8–11.
15. **Tortorella MD, Malfait AM, Deccico C, Arner E.** The role of ADAM-TS4 (aggrecanase-1) and ADAM-TS5 (aggrecanase-2) in a model of cartilage degradation. *Osteoarthritis Cartilage* 2001;9:539–552.
16. **Nishitani K, Ito H, Hiramitsu T, et al.** PGE2 inhibits MMP expression by suppressing MKK4-JNK MAP kinase-c-JUN pathway via EP4 in human articular chondrocytes. *J Cell Biochem* 2010;109:425–433.
17. **Kunisch E, Jansen A, Kojima F, et al.** Prostaglandin E2 differentially modulates proinflammatory/prodestructive effects of TNF-alpha on synovial fibroblasts via specific E prostanoid receptors/cAMP. *J Immunol* 2009;183:1328–1336.
18. **Attur M, Al-Mussawir HE, Patel J, et al.** Prostaglandin E2 exerts catabolic effects in osteoarthritis cartilage: evidence for signaling via the EP4 receptor. *J Immunol* 2008;181:5082–5088.
19. **Mbalaviele G, Pauley AM, Shaffer AF, et al.** Distinction of microsomal prostaglandin E synthase-1 (mPGES-1) inhibition from cyclooxygenase-2 inhibition in cells using a novel, selective mPGES-1 inhibitor. *Biochem Pharmacol* 2010;79:1445–1454.
20. **Tsutsumi R, Ito H, Hiramitsu T, et al.** Celecoxib inhibits production of MMP and NO via down-regulation of NF-kappaB and JNK in a PGE2 independent manner in human articular chondrocytes. *Rheumatol Int* 2008;28:727–736.
21. **Mastbergen SC, Bijlsma JW, Lafeber FP.** Selective COX-2 inhibition is favorable to human early and late-stage osteoarthritic cartilage: a human in vitro study. *Osteoarthritis Cartilage* 2005;13:519–526.
22. **Akamine Y, Kakudo K, Kondo M, et al.** Prolonged matrix metalloproteinase-3 high expression after cyclic compressive load on human synovial cells in three-dimensional cultured tissue. *Int J Oral Maxillofac Surg* 2012;41:874–881.
23. **Muroi Y, Kakudo K, Nakata K.** Effects of compressive loading on human synovium-derived cells. *J Dent Res* 2007;86:786–791.
24. **Kojima F, Naraba H, Miyamoto S, et al.** Membrane-associated prostaglandin E synthase-1 is upregulated by proinflammatory cytokines in chondrocytes from patients with osteoarthritis. *Arthritis Res Ther* 2004;6:R355–R365.
25. **Grimmer C, Pfander D, Swoboda B, et al.** Hypoxia-inducible factor 1alpha is involved in the prostaglandin metabolism of osteoarthritic cartilage through up-regulation of microsomal prostaglandin E synthase 1 in articular chondrocytes. *Arthritis Rheum* 2007;56:4084–4094.
26. **Ando W, Tateishi K, Katakai D, et al.** In vitro generation of a scaffold-free tissue-engineered construct (TEC) derived from human synovial mesenchymal stem cells: biological and mechanical properties and further chondrogenic potential. *Tissue Eng Part A* 2008;14:2041–2049.
27. **Takahashi I, Nuckolls GH, Takahashi K, et al.** Compressive force promotes sox9, type II collagen and aggrecan and inhibits IL-1beta expression resulting in chondrogenesis in mouse embryonic limb bud mesenchymal cells. *J Cell Sci* 1998;111(Pt14):2067–2076.
28. **Hunter CJ, Mouw JK, Levenston ME.** Dynamic compression of chondrocyte-seeded fibrin gels: effects on matrix accumulation and mechanical stiffness. *Osteoarthritis Cartilage* 2004;12:117–130.
29. **Fitzgerald JB, Jin M, Dean D, et al.** Mechanical compression of cartilage explants induces multiple time-dependent gene expression patterns and involves intracellular calcium and cyclic AMP. *J Biol Chem* 2004;279:19502–19511.
30. **Vincent TL, Hermansson MA, Hansen UN, Amis AA, Saklatvala J.** Basic fibroblast growth factor mediates transduction of mechanical signals when articular cartilage is loaded. *Arthritis Rheum* 2004;50:526–533.

31. **Abramson SB, Attur M.** Developments in the scientific understanding of osteoarthritis. *Arthritis Res Ther* 2009;11:227.
32. **Sah RL, Kim YJ, Doong JY, et al.** Biosynthetic response of cartilage explants to dynamic compression. *J Orthop Res* 1989;7:619–636.
33. **Sah RL, Doong JY, Grodzinsky AJ, Plaas AH, Sandy JD.** Effects of compression on the loss of newly synthesized proteoglycans and proteins from cartilage explants. *Arch Biochem Biophys* 1991;286:20–29.
34. **Kuettner KE, Cole AA.** Cartilage degeneration in different human joints. *Osteoarthritis Cartilage* 2005;13:93–103.
35. **Levick JR, McDonald JN.** Ultrastructure of transport pathways in stressed synovium of the knee in anaesthetized rabbits. *J Physiol* 1989;419:493–508.
36. **Schett G, Tohidast-Akrad M, Steiner G, Smolen J.** The stressed synovium. *Arthritis Res* 2001;3:80–86.
37. **Sasazaki Y, Seedhom BB, Shore R.** Morphology of the bovine chondrocyte and of its cytoskeleton in isolation and in situ: are chondrocytes ubiquitously paired through the entire layer of articular cartilage? *Rheumatology (Oxford)* 2008;47:1641–1646.
38. **Lin Z, Willers C, Xu J, Zheng MH.** The chondrocyte: biology and clinical application. *Tissue Eng* 2006;12:1971–1984.
39. **Cukierman E, Pankov R, Stevens DR, Yamada KM.** Taking cell-matrix adhesions to the third dimension. *Science* 2001;294:1708–1712.
40. **Schmeichel KL, Bissell MJ.** Modeling tissue-specific signaling and organ function in three dimensions. *J Cell Sci* 2003;116(Pt12):2377–2388.
41. **Hwang NS, Kim MS, Sampattavanich S, et al.** Effects of three-dimensional culture and growth factors on the chondrogenic differentiation of murine embryonic stem cells. *Stem Cells* 2006;24:284–291.
42. **Simon LS, Lanza FL, Lipsky PE, et al.** Preliminary study of the safety and efficacy of SC-58635, a novel cyclooxygenase 2 inhibitor: efficacy and safety in two placebo-controlled trials in osteoarthritis and rheumatoid arthritis, and studies of gastrointestinal and platelet effects. *Arthritis Rheum* 1998;41:1591–1602.
43. **Mitchell JA, Akarasereenont P, Thiemermann C, Flower RJ, Vane JR.** Selectivity of nonsteroidal antiinflammatory drugs as inhibitors of constitutive and inducible cyclooxygenase. *Proc Natl Acad Sci U S A* 1993;90:11693–11697.
44. **Koyama Y, Mizobata T, Yamamoto N, et al.** Endothelins stimulate expression of cyclooxygenase 2 in rat cultured astrocytes. *J Neurochem* 1999;73:1004–1011.
45. **Kujubu DA, Herschman HR.** Dexamethasone inhibits mitogen induction of the TIS10 prostaglandin synthase/cyclooxygenase gene. *J Biol Chem* 1992;267:7991–7994.
46. **Shimpo H, Sakai T, Kondo S, et al.** Regulation of prostaglandin E(2) synthesis in cells derived from chondrocytes of patients with osteoarthritis. *J Orthop Sci* 2009;14:611–617.
47. **Rai MF, Rachakonda PS, Manning K, et al.** Quantification of cytokines and inflammatory mediators in a three-dimensional model of inflammatory arthritis. *Cytokine* 2008;42:8–17.
48. **Scott I, Midha A, Rashid U, et al.** Correlation of gene and mediator expression with clinical endpoints in an acute interleukin-1beta-driven model of joint pathology. *Osteoarthritis Cartilage* 2009;17:790–797.
49. **Wood DD, Ihrie EJ, Dinarello CA, Cohen PL.** Isolation of an interleukin-1-like factor from human joint effusions. *Arthritis Rheum* 1983;26:975–983.
50. **Saha N, Moldovan F, Tardif G, et al.** Interleukin-1beta-converting enzyme/caspase-1 in human osteoarthritic tissues: localization and role in the maturation of interleukin-1beta and interleukin-18. *Arthritis Rheum* 1999;42:1577–1587.
51. **Clements KM, Price JS, Chambers MG, et al.** Gene deletion of either interleukin-1beta, interleukin-1beta-converting enzyme, inducible nitric oxide synthase, or stromelysin 1 accelerates the development of knee osteoarthritis in mice after surgical transection of the medial collateral ligament and partial medial meniscectomy. *Arthritis Rheum* 2003;48:3452–3463.
52. **Kokebie R, Aggarwal R, Lidder S, et al.** The role of synovial fluid markers of catabolism and anabolism in osteoarthritis, rheumatoid arthritis and asymptomatic organ donors. *Arthritis Res Ther* 2011;13:R50.
53. **Neu CP, Reddi AH, Komvopoulos K, Schmid TM, Di Cesare PE.** Increased friction coefficient and superficial zone protein expression in patients with advanced osteoarthritis. *Arthritis Rheum* 2010;62:2680–2687.
54. **Kido S, Kuriwaka-Kido R, Umino-Miyatani Y, et al.** Mechanical stress activates Smad pathway through PKCδ to enhance interleukin-11 gene transcription in osteoblasts. *PLoS One* 2010;5:13090.
55. **Turner NJ, Jones HS, Davies JE, Canfield AE.** Cyclic stretch-induced TGFbeta1/Smad signaling inhibits adipogenesis in umbilical cord progenitor cells. *Biochem Biophys Res Commun* 2008;377:1147–1151.
56. **Hsu HJ, Lee CF, Locke A, Vanderzyl SQ, Kaunas R.** Stretch-induced stress fiber remodeling and the activations of JNK and ERK depend on mechanical strain rate, but not FAK. *PLoS One* 2010;5:12470.
57. **Glossop JR, Cartmell SH.** Effect of fluid flow-induced shear stress on human mesenchymal stem cells: differential gene expression of IL1B and MAP3K8 in MAPK signaling. *Gene Expr Patterns* 2009;9:381–388.
58. **Wang BW, Chang H, Shyu KG.** Regulation of resistin by cyclic mechanical stretch in cultured rat vascular smooth muscle cells. *Clin Sci (Lond)* 2009;118:221–230.
59. **Kitase Y, Barragan L, Qing H, et al.** Mechanical induction of PGE2 in osteocytes blocks glucocorticoid-induced apoptosis through both the β-catenin and PKA pathways. *J Bone Miner Res* 2010;25:2657–2668.
60. **Olkku A, Leskinen JJ, Lammi MJ, Hynynen K, Mahonen A.** Ultrasound-induced activation of Wnt signaling in human MG-63 osteoblastic cells. *Bone* 2010;47:320–330.
61. **Liedert A, Wagner L, Seefried L, et al.** Estrogen receptor and Wnt signaling interact to regulate early gene expression in response to mechanical strain in osteoblastic cells. *Biochem Biophys Res Commun* 2010;394:755–759.

Funding statement:

- This study was supported by a grant from 'Knowledge Cluster Initiative' to K. Nakata from The Ministry of Education, Culture, Sports, Science and Technology (MEXT) and Grants-in-Aid for Scientific Research (#23390363 (B)).

Author contributions:

- K. Shimomura: Data collection, Data analysis, Writing the paper
- T. Kanamoto: Data analysis
- K. Kita: Data analysis
- Y. Akamine: Data analysis
- N. Nakamura: Data analysis
- T. Mae: Data analysis
- H. Yoshikawa: Data analysis
- K. Nakata: Data collection, Data analysis, Writing the paper

ICMJE Conflict of Interest:

- None declared

FEBS Letters xxx (2015) xxx–xxx

ELSEVIER

FEBS Letters

journal homepage: www.FEBSLetters.org

Hyaluronan inhibits BMP-induced osteoblast differentiation

Keiko Kaneko [a], Chikahisa Higuchi [a], Yasuo Kunugiza [a], Kiyoshi Yoshida [a], Takashi Sakai [a], Hideki Yoshikawa [a], Ken Nakata [a,b,*]

[a] Department of Orthopedic Surgery, Osaka University Graduate School of Medicine, 2-2 Yamada-oka, Suita, Osaka 565-0871, Japan
[b] Medicine for Sports and Performing Arts, Department of Health and Sport Sciences, Osaka University Graduate School of Medicine, 2-2 Yamada-oka, Suita, Osaka 565-0871, Japan

ARTICLE INFO

Article history:
Received 23 July 2014
Revised 22 November 2014
Accepted 30 December 2014
Available online xxxx

Edited by Zhijie Chang

Keywords:
Hyaluronan
CD44
Osteoblast
Bone morphogenetic protein

ABSTRACT

Hyaluronan (HA), one of the major structural extracellular components in cartilage, regulates cellular responses via receptors such as CD44. However, the direct effects of HA on osteoblastic differentiation has not been studied in detail. Here, we investigated the effects of HA (molecular weight: 900–1200kDa) on osteoblastic differentiation that was induced by bone morphogenetic protein (BMP) in C2C12 cells (mouse myoblastic cells) and ST2 cells (mouse bone marrow cells). BMP-induced osteoblastic differentiation and Smad1/Smad5/Smad8 phosphorylation were downregulated by HA. Use of the CD44-blocking antibody restored HA-induced inhibition of osteoblastic differentiation and Smad1/Smad5/Smad8 phosphorylation. Our results indicate that HA inhibits BMP-induced osteoblastic differentiation through the CD44 receptor.

1. Introduction

Hyaluronan (HA) is a linear polymer, which is characterized by repeated disaccharide units of D-glucuronate and N-acetyl-D-glucosamine [1,2]. HA is a major component of the extracellular matrix of cartilage, which regulates cell proliferation, differentiation, motility, and adhesion directly via receptors such as CD44 [2,3]. In addition to being expressed by many cell types [4,5], CD44 is one of the major HA receptors. HA participates in many functions via the CD44 receptor such as regulation of cartilage metabolism, including osteoclastogenesis [6–8]. However, the direct effects of HA on osteoblastic differentiation have rarely been studied [9].

Bone morphogenetic protein-2 (BMP-2), a member of the transforming growth factor-β superfamily, was originally identified as an inducer of ectopic bone formation [10]. BMP-2 is known to play important roles in bone formation, bone regeneration [11], fracture healing [12], and osteophyte formation [13]. The binding of BMP-2 to type I and II serine/threonine kinase receptors induces Smad phosphorylation. Phosphorylated Smads then translocate from the cytoplasm to the nucleus to regulate the transcription of various genes, such as alkaline phosphatase (ALP), runt-related transcription factor 2 (Runx2), and osteocalcin [14]. BMP-2 also serves as a useful experimental model of osteoblastic differentiation in vitro because undifferentiated mesenchymal cells, myoblasts, or osteoprogenitor cells can be differentiated into osteoblasts by BMP-2 [15].

In this study, we investigated the effects of HA on bone formation using BMP-induced osteoblastic differentiation in mouse myoblast cells (C2C12 cells) and mouse bone marrow cells (ST2 cells). These cells differentiate into osteoblasts after treatment with BMP-2 as well as primary osteoblasts and they are known to be models for the study of osteoblast differentiation [16,17]. We examined whether the major receptor for HA, CD44, is involved in BMP-induced osteoblastic differentiation. Furthermore, we investigated the potential crosstalk between HA–CD44 and BMP–Smad signaling.

2. Methods

2.1. Cell culture

The experimental design of the study is summarized in Fig. 1. C2C12 and ST2 cells were obtained from Riken Cell Bank (Tsukuba, Japan). C2C12 cells were maintained in Dulbecco's modified Eagle's medium (Invitrogen, Carlsbad, CA, USA) containing 10% fetal bovine serum (FBS; Hyclone, Road Logan, UT, USA). ST2 cells were maintained in RPMI 1640 (Invitrogen) containing 10% FBS in a humidified atmosphere of 5% CO_2 at 37 °C. C2C12 cells were treated with HA at different concentrations in the presence of 300 ng/

* Corresponding author at: Medicine for Sports and Performing Arts, Department of Health and Sport Sciences, Osaka University Graduate School of Medicine, 2-2 Yamada-oka, Suita, Osaka 565-0871, Japan. Fax: +81 6 6210 8438.
E-mail address: ken-nakata@umin.ac.jp (K. Nakata).

http://dx.doi.org/10.1016/j.febslet.2014.12.031
0014-5793/

Please cite this article in press as: Kaneko, K., et al. Hyaluronan inhibits BMP-induced osteoblast differentiation. FEBS Lett. (2015), http://dx.doi.org/10.1016/j.febslet.2014.12.031

ml rhBMP-2 (Osteopharma Inc., Osaka, Japan). ST2 cells were transferred to growth medium supplemented with 0.1 mM ascorbic acid (Sigma–Aldrich, St. Louis, MO, USA) and 4 mM β-glycerophosphate (Sigma–Aldrich), and treated with HA at different concentrations in the presence of 100 ng/ml rhBMP-2.

2.2. Immunocytochemistry

To examine CD44 expression, C2C12 and ST2 cells were plated on chamber slides and fixed with 4% paraformaldehyde for 30 min, blocked with 1% bovine serum albumin (BSA; Sigma–Aldrich) for 1 h, incubated overnight with a primary antibody at 4 °C, and then incubated for 1 h with a fluorescein isothiocyanate (FITC)-conjugated secondary antibody. The primary antibody was anti-CD44 monoclonal antibody [Becton, Dickinson & Co (BD), Franklin Lakes, NJ, USA]. The clone used for the anti-CD44 monoclonal antibody was IM7.

2.3. Flow cytometry (FACS)

Cells were scraped gently and washed with phosphate-buffered saline (PBS). Approximately 5×10^5 cells were suspended in Hank's balanced salt solution containing 1% BSA on ice. Cells were incubated on ice with APC anti-CD44 (BD Bioscience, Franklin Lakes, NJ USA) for 30 min. Fluorescence was measured using the BD FACSCanto™ II system.

2.4. Proliferation assay

Cells were cultured in 96-well plates at a density of $2 \times 10^4/cm^2$ with or without rhBMP-2 at concentrations of 300 ng/ml or 100 ng/ml and HA (Artz® from Seikagaku, Kogyo Co., Tokyo, Japan) at concentrations of 0, 50, 500, or 1000 μg/ml. After 3 days, cell proliferation was assessed using the Premix WST-1 Cell Proliferation Assay System (Takara Bio, Otsu, Japan), according to the manufacturer's instructions.

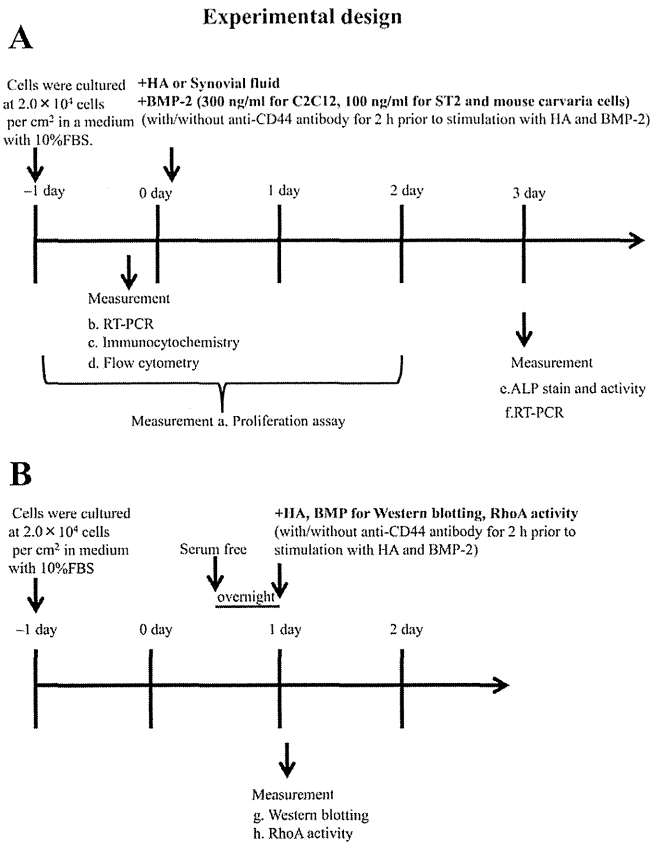

Fig. 1. Flow chart of the experimental design. For detailed description see the Section 2. All of the quantitative experiments were performed at least in triplicate and each experiment was performed a minimum of three times to consider the effects of biological variation.

2.5. ALP staining

Cells were plated on 24-well plates at a density of 2×10^4 cells/well. After 24 h, the culture medium was replaced with growth medium containing rhBMP-2 and HA at concentrations of 0, 50, 500, or, 1000 μg/ml, followed by culture for 3 days. Cells were washed with PBS and fixed for 15 min with 10% formalin at room temperature. After fixation, cells were incubated for 1 h at room temperature with the ProtoBlot® AP system and stabilized substrate (Promega, Madison, WI, USA).

2.6. ALP activity

To measure ALP activity, cells were washed with PBS and lysed in mammalian protein extraction reagent (M-PER; Pierce, Rockford, IL, USA), according to the manufacturer's instructions. ALP activity was measured using the LabAssay™ ALP system (Wako Pure Chemicals Industries Ltd., Osaka, Japan) with p-nitrophenyl phosphate as the substrate. To normalize the enzyme activity, the protein content was measured using a bicinchoninic acid protein assay kit (Pierce, Rockford, IL, USA).

2.7. Reverse transcription polymerase chain reaction and quantitative real-time polymerase chain reaction

Total RNA was isolated using TRIzol (Invitrogen) according to the manufacturer's instructions. cDNA was synthesized using the Transcriptor First Strand cDNA Synthesis Kit (Roche Diagnostics, Mannheim, Germany). RT-PCR was performed using PCR Master Mix (Promega) and the following primers: ALP, forward 5′-GCCCT CTCCAAGACATATA-3′ and reverse 5′-CCATGATCACGTCGATATCC-3′; Runx2, forward 5′-GCTTGATCACTCTAAACCTA-3′ and reverse 5′-AAAGCCGAGCTG CCAGAGCTT-3′; osterix, forward 5′-GAA-GAAGCTCACTATGGCTC-3′ and reverse 5′-GAAAAGCCAGTTGCA-GACGA-3′; osteocalcin, forward 5′-CAAGTCCCACACA GCAGCTT-3′ and reverse 5′-AAAGCCGAGCTGCCAGAGTT-3′; CD44, forward 5′-GCACCCCAGAAGGCTACATTT-3′ and reverse 5′-TCTGCCCA-CACCTTCTC CTACTAT-3′ [18]; and GAPDH, forward 5′-TGAACGG-GAAGCTCACTGG-3′ and reverse 5′-TCCACCACCTGTTGCTGTA-3′.The PCR products were separated by agarose gel electrophoresis and detected using ethidium bromide. We conducted real-time PCR using a Light Cycler system (Roche Applied Science, Basel, Switzerland). By using a Quantitect SYBR Green PCR Kit (Qiagen, Venlo, Limburg, The Netherlands), each cDNA sample was evaluated in triplicate reactions. Expression values were normalized to GAPDH. The following primers were used: ALP, forward 5′-AATCGGAACAACCTGACTGACC-3′ and reverse 5′-TCCTTCCAGCA-AGAAGAA-3′; Runx2, forward 5′-GCCCAGGCGTATTTCAGAT-3′ and reverse 5′-TGCCTGGCTCTTCTTACTGAG-3′; Osterix, forward 5′-AGGCACAAAGAAGCCATAC-3′ and reverse 5′-AATGAGTGAGG-GAAGGGT-3′; Osteocalcin, forward 5′-CTCACTCTGCTGGCCCTG-3′ and reverse 5′-CCGTAGATGCGTTTGTAGGC-3′; GAPDH, forward 5′-TGTCCGTCGTGGATCTGAC-3′ and reverse 5′-CCTGCTTCAC-CACCTTCTTG-3′.

2.8. Western blotting

The Smad signals were analyzed by monitoring the phosphorylation levels of receptor-activated Smads (Smad1, Smad5, and Smad8; Smad1/5/8). Cells were treated with 500 μg/ml HA in the

Please cite this article in press as: Kaneko, K., et al. Hyaluronan inhibits BMP-induced osteoblast differentiation. FEBS Lett. (2015), http://dx.doi.org/10.1016/j.febslet.2014.12.031

presence or absence of rhBMP-2 for 30 min. Next, cells were lysed rapidly on ice using Blue Loading Buffer Reagents (Cell Signaling Technology, Beverly, MA, USA) containing 0.125 M dithiothreitol. These samples were subjected to 4–12% sodium dodecyl sulfate–polyacrylamide gel electrophoresis and then transferred to nitrocellulose membranes (Bio-Rad Laboratories, Hercules, CA, USA). After blocking with 0.1% Tween 20 and PBS containing 3% BSA, the membranes were incubated with specific primary antibodies against phospho-Smad1/5/8, Smad1, or β-actin rabbit monoclonal antibodies (Cell Signaling Technology, Beverly, MA, USA). The membranes were incubated with horseradish peroxidase-conjugated secondary antibodies (GE Healthcare) and enhanced chemiluminescence (ECL) reagents (GE Healthcare).

2.9. RhoA activity

RhoA activity was assayed using rhotekin beads. Cells were treated with 500 μg/ml HA in the presence of rhBMP-2 for 30 min. RhoA activity assay was performed using the Rho Activation Assay Kit (Millipore, Billerica, MA, USA). Cells were lysed using lysis buffer, and the cell lysates were clarified by centrifugation, before incubation with Rho Assay Reagent for 45 min to selectively bind the activated RhoA in a pull-down assay. Whole-cell lysates were immunoblotted directly to determine the total amount of RhoA, where RhoA was detected by Western blotting.

2.10. Neutralization studies using anti-CD44 antibody

Cells were pretreated with CD44-blocking antibody for 2 h before stimulation with different concentrations of HA in the presence of rhBMP-2. Anti-CD44-blocking rat antibody (Calbiochem, San Diego, CA, USA) [19] was used in the neutralization assay for ALP staining, ALP activity analysis, Western blotting, as well as to determine RhoA activity. The clone used for anti-CD44 blocking was A020. Rat IgG antibody was used as the negative control, which was purchased from Santa Cruz Biotechnology (Dallas, TX, USA).

2.11. Effects of synovial fluid on osteoblastic differentiation

The effects of human synovial fluids on osteoblastic differentiation were studied by evaluating ALP activity. Synovial fluid samples were obtained from patients in the Department of Orthopedic Surgery at Osaka University. Written informed consent was obtained from each patient and the study was approved by the Ethical Committee of Osaka University Graduate School of Medicine. Six samples were obtained from three patients with severe osteoarthritis (OA) and three patients with traumatic arthritis (TA). The HA concentrations of all samples were determined using an ELISA kit (Seikagaku, Kogyo Co., Tokyo, Japan).

C2C12 cells were plated on 24-well plates at a density of 2×10^4 cells/well in 500 μl of medium. To test the effects of synovial fluid, 50 μl of the synovial fluid from the patients and 300 ng/ml rhBMP-2 were added to the culture medium at 24 h after plating. The controls were not treated with synovial fluid. After culture for 3 days, ALP activity was measured using the Lab Assay™ ALP system (Wako Pure Chemicals Industries Ltd.).

2.12. Effects of HA on ALP activity in mouse calvaria cells

Mouse primary osteoblasts were isolated from the calvariae of 3-day-old C57BL/6 mice (Charles River Laboratories Japan, Inc., Osaka, Japan) by sequential collagenase digestion, as described previously [20]. Cells were cultured in α-minimum essential medium (Invitrogen) containing 10% FBS, 0.1 mM ascorbic acid (Sigma–Aldrich), and 4 mM β-glycerophosphate (Sigma–Aldrich). Cells were treated with HA at concentrations of 0, 500, and 1000 μg/ml in the presence of 100 ng/ml rhBMP-2. After culture for 3 days, ALP activity was measured using the Lab Assay™ ALP system (Wako Pure Chemicals Industries Ltd.). The animal experimental protocol was approved by the Ethics Review Committee for animal experimentation of Osaka University School of Medicine.

2.13. Statistical analysis

All experiments were repeated at least three times. Data were expressed as the mean ± standard deviation and analyzed by one-way analysis of variance (ANOVA), followed by Dunnett's test if significant differences were detected. Differences between groups were considered significant at $P < 0.05$.

3. Results

3.1. Expression of CD44 receptors on C2C12 and ST2 cells

Using semiquantitative RT-PCR, we clearly detected the expression of CD44 mRNA in C2C12 and ST2 cells, which corresponded to 300 base pairs (Fig. 2A). CD44 receptors were identified by immunocytochemistry with green labeling, which made the cytoplasm visible in the C2C12 (Fig. 2)B-a and ST2 (Fig. 2)B-b cells. In addition, we used FACS to observe the temporal expression of CD44 receptors on the surfaces of C2C12 and ST2 cells. The purity of the CD44-positive cells was 80.3 ± 0.1% in C2C12 cells and 87.9 ± 0.1% in ST2 cells (Fig. 2C).

3.2. Effects of HA on osteoblastic differentiation in C2C12 and ST2 cells based on the CD44 receptor

HA did not affect the proliferation of C2C12 (Fig. 3A) or ST2 (data not shown) cells. Fig. 3B shows that HA significantly reduced

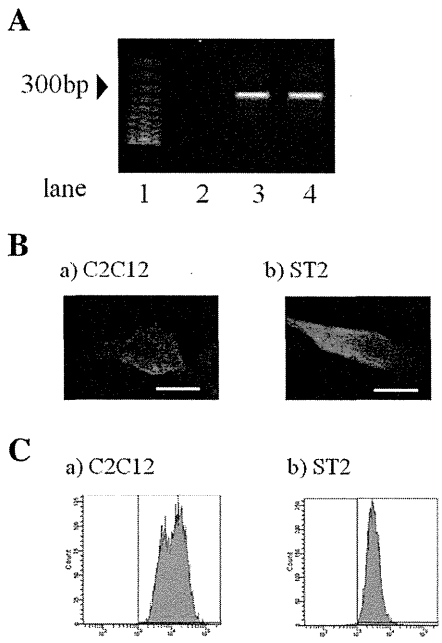

Fig. 2. CD44 expression in C2C12 and ST2 cells. (A) RT-PCR of the mRNA of the CD44 gene. Lane 1: DNA ladder, lane 2: negative control, lane 3: C2C12 cells, lane 4: ST2 cells. (B) Representative example of CD44 protein expression in C2C12 cells and ST2 cells: (a) C2C12 cells; (b) ST2 cells. Counterstaining with DAPI (blue) and CD44 (green), scale bar = 20 μm. (C) CD44 expression in C2C12 and ST2 cells based on flow cytometry: (a) C2C12 cells; (b) ST2 cells. (For interpretation of the references to color in this figure legend, the reader is referred to the web version of this article.)

Please cite this article in press as: Kaneko, K., et al. Hyaluronan inhibits BMP-induced osteoblast differentiation. FEBS Lett. (2015), http://dx.doi.org/10.1016/j.febslet.2014.12.031

ALP staining and activity in C2C12 cells treated with HA at concentrations of 50, 500, and 1000 μg/ml (14.15 ± 0.39, 95% CI 13.17–15.12, $P = 0.038$, 10.80 ± 0.73, 95% CI 8.98–12.63, $P = 0.0005$, and 10.89 ± 0.44, 95% CI 8.98–11.19, $P = 0.0004$ vs control, 19.05 ± 0.61, 95% CI 17.52–20.59 respectively). Fig. 4A shows that HA significantly reduced ALP staining and activity in ST2 cells with HA concentrations of 500 and 1000 μg/ml (14.04 ± 1.30, 95% CI 10.78–17.29, $P = 0.0238$ and 10.33 ± 0.66, 95% CI 8.67–11.99, $P = 0.0001$ vs control, 16.45 ± 0.78, 95% CI 14.50–18.41 respectively). Furthermore, the semiquantitative RT-PCR and real-time PCR revealed that ALP and Runx2 mRNA expression was suppressed at HA concentrations of 500 and 1000 μg/ml (Figs. 3D, F and 4C, E). ALP staining and activity were restored by adding CD44-blocking antibody compared to that in untreated cells (Fig. 3C: 0 μg/ml, 16.45 ± 0.78, 95% CI 14.50–18.41; 50 μg/ml, 15.05 ± 0.51, 95% CI 13.77–16.34, $P = 0.9939$; 500 μg/ml, 14.04 ± 1.30, 95% CI 10.78–17.29, $P = 0.6683$; 1000 μg/ml, 10.33 ± 0.6683, 95% CI 8.67–11.99, $P = 0.8913$; Fig. 4B: 0 μg/ml, 14.39 ± 1.31, 95% CI 11.11–17.66; 50 μg/ml, 14.76 ± 1.91, 95% CI 10.00–19.52, $P = 0.9714$; 500 μg/ml, 14.07 ± 0.64, 95% CI 12.46–15.67, $P = 0.9810$; 1000 μg/ml, 13.28 ± 1.04, 95% CI 10.68–15.88, $P = 0.6235$). RT-PCR and real-time PCR showed that the CD44-blocking antibody failed to suppress mRNA expression of any genes, including ALP and Runx2 (Figs. 3E, G and 4D, F).

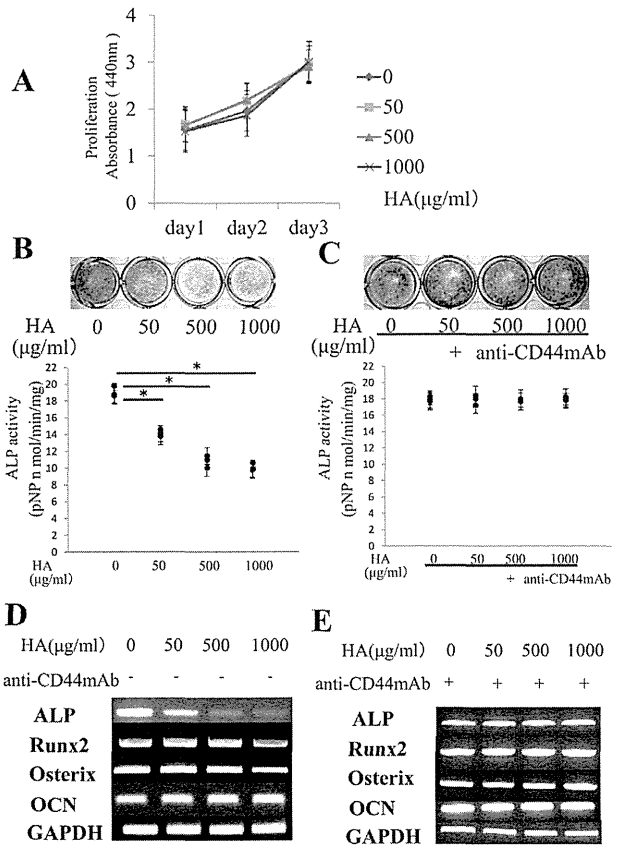

Fig. 3. Effects of HA on osteoblast differentiation in C2C12 cells. (A) Effects on cell proliferation. (B) and (C) Effects of HA on ALP staining and activity. (B) Non-treated cells; (C) cells treated with 5 μg/ml CD44-blocking antibody. (D) and (E) Effects of HA on osteoblast-related genes on RT-PCR. (D) Non-treated cells; (E) cells treated with 5 μg/ml CD44-blocking antibody. (F) and (G) Effects of HA on osteoblast-related genes on real-time PCR. (F) Non-treated cells; (G) cells treated with 5 μg/ml CD44-blocking antibody. The asterisks indicate $P < 0.05$ compared with the control without any treatment.

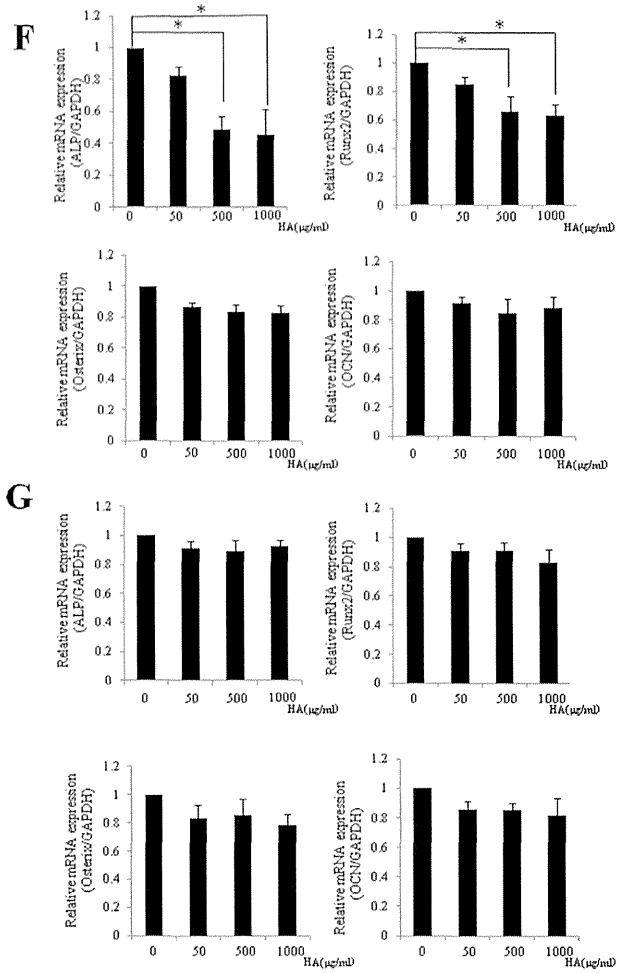

Fig. 3 (*continued*)

3.3. Effect of HA on the downregulation of Smad1/5/8 phosphorylation via CD44 receptor signaling

We investigated the molecular mechanism underlying the inhibition of BMP signal transduction by HA. Smad signals were analyzed by monitoring the phosphorylation levels of a set of receptor-activated Smads (Smad1, Smad5, and Smad8; Smad1/5/8). The cells were treated with HA (500 μg/ml) in the presence or absent of rhBMP-2. The phosphorylation of Smad1/5/8 by rhBMP-2 was downregulated. When the cells were treated with CD44-blocking antibody, the phosphorylation level of Smad1/5/8 was rescued as compared with the untreated cells (Fig. 5A, Suppl. Fig. 1A). The protein level of total Smad1/5/8 was increased in lines b and c because BMP accelerated the Smad pathway. In contrast, the protein level of total Smad1/5/8 was decreased by adding CD44-blocking antibody. Reports of a previous study indicated that CD44 modulates Smad1 activation in the BMP signaling pathway [7]. In our experiment, CD44-blocking antibody may have an effect on the protein level of total Smad1/5/8 through the CD44–Smad interaction. These results demonstrate that CD44 is involved in the phosphorylation of Smad1/5/8 by rhBMP-2.

3.4. Activation of Rho A by HA via CD44 receptors

We measured the activity of RhoA activity by rhotekin beads in the cells. The level of active GTP-bound RhoA increased after the addition of 500 μg/ml HA.

Please cite this article in press as: Kaneko, K., et al. Hyaluronan inhibits BMP-induced osteoblast differentiation. FEBS Lett. (2015), http://dx.doi.org/10.1016/j.febslet.2014.12.031

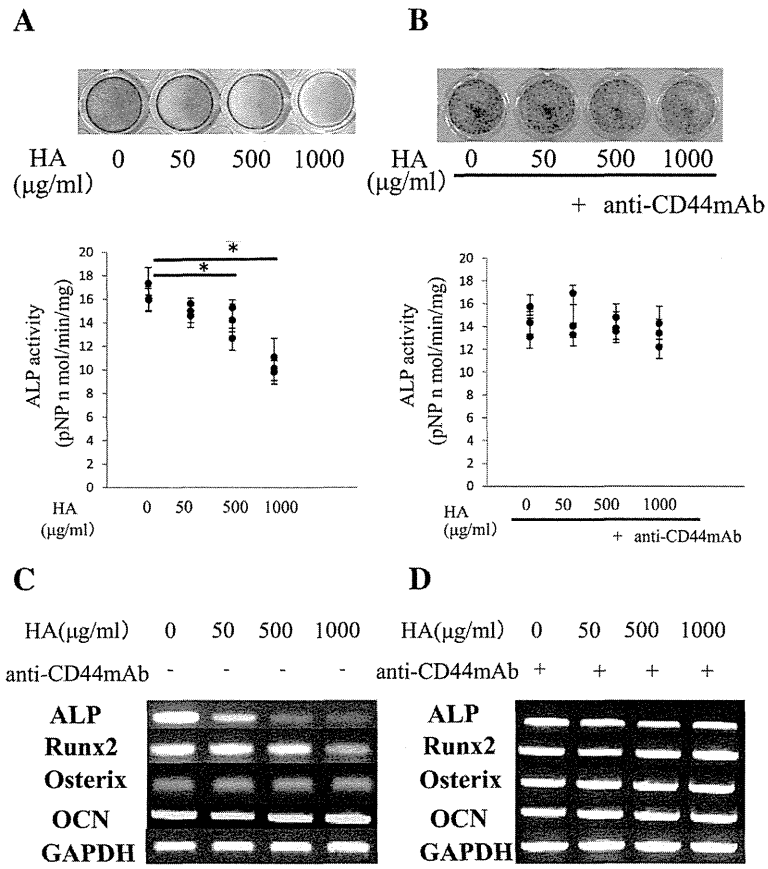

Fig. 4. Effects of HA on osteoblast differentiation in ST2 cells. (A) and (B) Effects of HA on ALP staining and activity. (A) Non-treated cells; (B) cells treated with 5 μg/ml CD44-blocking antibody. (C) and (D) Effects of HA on osteoblast-related genes on RT-PCR. (C) Non-treated cells; (D) cells treated with 5 μg/ml CD44-blocking antibody. (E) and (F) Effects of HA on osteoblast-related genes on real-time PCR. (E) Non-treated cells; (F) cells treated with 5 μg/ml CD44-blocking antibody. The asterisks indicate differences where $P < 0.05$ compared with the control without any treatment.

Next, the cells were pretreated with 5 μg/ml CD44-blocking antibody. The level of RhoA activity decreased as compared with the untreated cells (Fig. 5B, Suppl. Fig. 1B).

3.5. Effects of human synovial fluid on BMP-induced osteoblastic differentiation

Fig. 6B summarizes the clinical information and HA concentrations of the patients who received synovial fluid. HA concentrations varied between 1.7 and 2.2 mg/ml. To study the effects of synovial fluid on osteoblastic differentiation, we obtained HA concentrations of 50 μl from the synovial fluids of patients, which corresponded to the significant ranges observed in the present study. Treatment with human synovial fluid strongly suppressed ALP activity in C2C12 cells (Fig. 6A). ALP activity was significantly lower than that of the control (control, 14.41 ± 0.89, 95% CI 12.19–16.63; No. 1, 4.85 ± 0.20, 95% CI 4.34–5.37, $P < 0.05$; No. 2, 5.61 ± 0.34, 95% CI 4.76–6.46, $P < 0.05$; No. 3, 6.54 ± 0.52, 95% CI 5.23–7.86, $P < 0.05$; No. 4, 4.92 ± 0.11, 95% CI 4.63–5.20; No. 5, 5.16 ± 0.34, 95% CI 4.31–6.01, $P < 0.05$; No. 6, 6.83 ± 0.35, 95% CI 5.94–7.73, $P < 0.05$). There was little difference in ALP activity of the synovial fluid from patients with OA (No. 1, No. 2, and No. 3) and those with trauma (No. 4, No. 5, and No. 6).

3.6. Effects of HA on BMP-induced osteoblastic differentiation in mouse calvaria cells

We tested mouse calvaria cells. The cells were treated with HA at different concentrations in the presence of rhBMP-2 (100 ng/ml). HA significantly reduced the activity of ALP at an HA concentration of 500 and 1000 μg/ml ($P = 0.0087$ and $P = 0.0006$ vs control, respectively; Fig. 7A). Furthermore, the activity of ALP was restored by adding CD44-blocking antibody (10 μg/ml), as compared with the untreated cells ($P = 0.1935$ and $P = 0.0717$ vs control, respectively; Fig. 7B).

4. Discussion

In this study, we found that HA inhibited BMP-induced osteoblastic differentiation in C2C12 and ST2 cells. Similar effects of HA during BMP-induced osteoblastic differentiation were observed in mouse calvaria cells. We also investigated the signal transduction of HA inhibition during osteoblastic differentiation and observed that CD44-blocking antibody restored the HA-mediated downregulation of Smad1/5/8 phosphorylation and HA inhibition during osteoblastic differentiation.

We also tested the BMP reporter assay in C2C12 cells. A luciferase reporter plasmid driven by the Id1 promoter (Id1WT4F-luc) was provided by Dr. Katagiri (Saitama Medical School, Saitama, Japan) [21,22]. We assayed the effect of HA addition on the activity of a luciferase reporter with an Id1 promoter. Id1 is known to be an early response gene to BMP-2 and to contain both a BMP-responsive element (BRE) and a cAMP-response element (CRE). The elevation of luciferase activity in C2C12 cells in response to BMP-2 treatment was further downregulated by the addition of HA, indicating that HA decelerates BMP signaling (Suppl. Fig. 2).

Many recent studies have focused on HA-mediated CD44 interactions with downstream effectors. For example, Rho GTPase

Please cite this article in press as: Kaneko, K., et al. Hyaluronan inhibits BMP-induced osteoblast differentiation. FEBS Lett. (2015), http://dx.doi.org/10.1016/j.febslet.2014.12.031

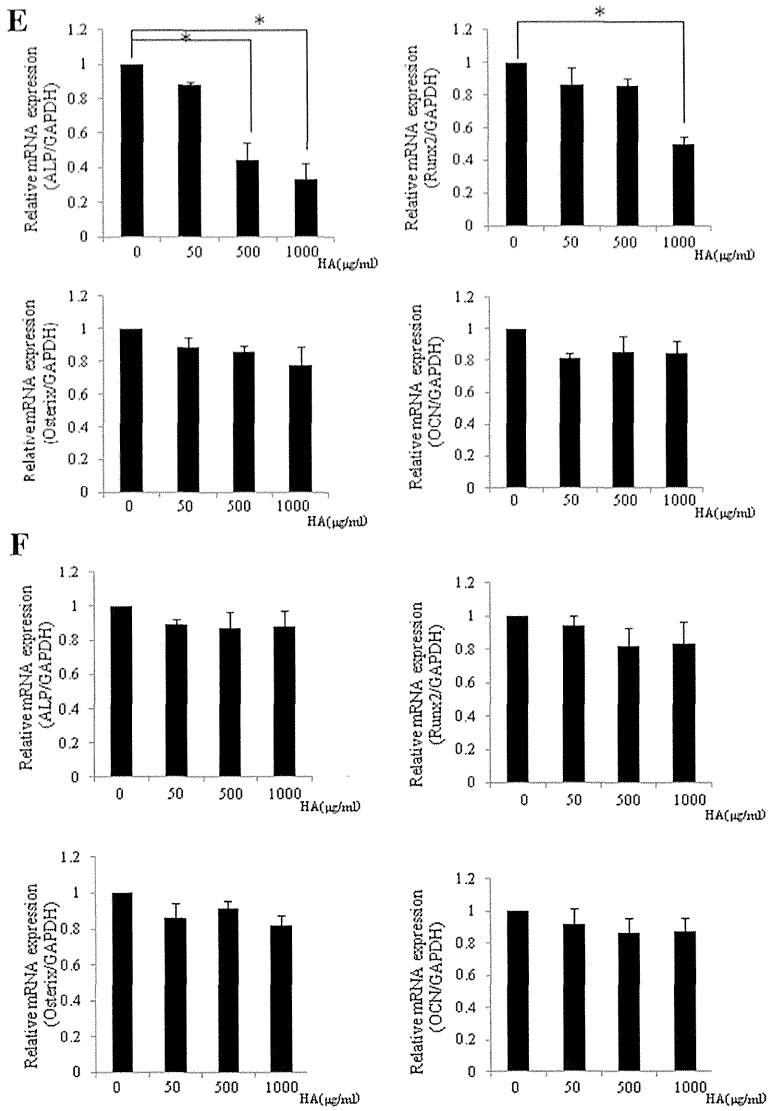

Fig. 4 (*continued*)

signaling was shown to be mediated via HA–CD44 interaction in tumor cells [4,23,24]. Rho GTPases (RhoA, Rac1, and Cdc42) are members of the Rho subclass of the Ras superfamily [25]. In addition, recent findings indicate that the RhoA signaling pathway has important roles in bone remodeling. For example, in osteoblast survival [26], the integrity of the actin cytoskeleton as well as migration [27] and differentiation [28–30] are regulated by RhoA signaling. We examined the effects of HA on RhoA activation in cells. We found that HA activated RhoA, whereas a CD44-blocking antibody inhibited this activation.

In the present study, it was unclear whether HA enhanced RhoA activation in cells, whether RhoA activation affected BMP signal transduction directly or whether the suppression of BMP-induced osteoblastic differentiation was mediated via other signaling pathways modulated by HA. Therefore, further research is needed to examine the molecular mechanisms, including the correlations between HA and other receptors.

We also found that human synovial fluid negatively regulated BMP-induced osteoblastic differentiation in vitro. We analyzed the molecular size of synovial fluid HA, which was approximately 50–2000kDa (data not shown). The synovial fluid of our samples contained various sizes of HA compared to Artz (900–1200kDa). In this study, we detected no differences in ALP activity in the synovial fluid samples, although the size or viscosity of the components could have affected the biological activity of HA. In human synovial fluid, many other components may have relevant biological activities in human synovial fluid [31]. In our future study, other components in addition to HA should be examined.

Clinically, intra-articular HA injection is one of the treatment of osteoarthritis (OA) [32]. HA contributes to the lubrication, shock absorption, hydration, and nutrition of the joint tissue, as well as to articular cartilage formation and repair [33]. OA is a chronic degenerative joint disorder, which is characterized by articular cartilage destruction and bone formation such as osteophyte formation and subchondral bone screlosis [34,35]. Since it has been reported that HA concentration of the joint is reduced in OA patients [36], HA may have therapeutic significance in OA patient by inhibiting bone formation.

In conclusion, HA negatively regulates BMP-induced osteoblastic differentiation via the CD44 receptor, suggesting that HA may have a significant role in bone metabolism in the progression of OA.

Please cite this article in press as: Kaneko, K., et al. Hyaluronan inhibits BMP-induced osteoblast differentiation. FEBS Lett. (2015), http://dx.doi.org/10.1016/j.febslet.2014.12.031

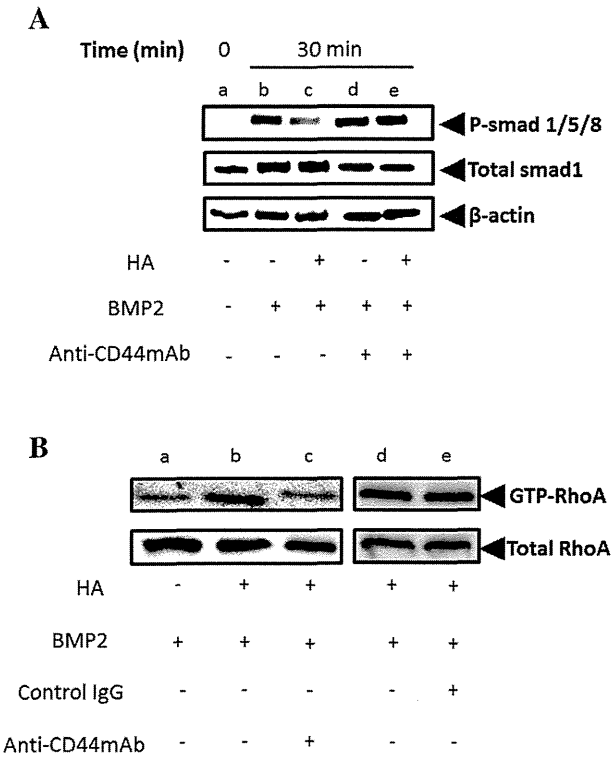

Fig. 5. Effects of HA via CD44 on Smad1/5/8 phosphorylation and the activation of RhoA in C2C12 cells. (A) Effects of HA via CD44 on Smad1/5/8 phosphorylation. (a, b, c: non-treated cells; d, e: cells treated with 5 μg/ml CD44-blocking antibody). (B) Activation of RhoA by HA via CD44. (a, b, d: non-treated cells; c; cells treated with 5 μg/ml CD44-blocking antibody; e: cells treated with control IgG). Each experiment was performed a minimum of three times.

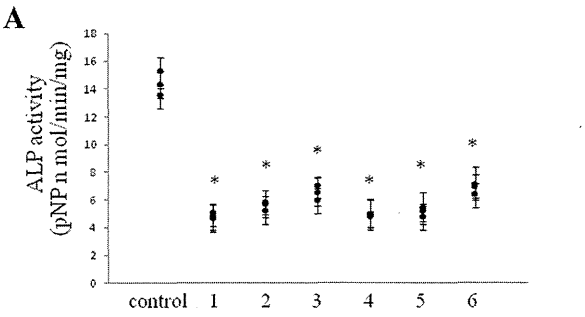

B

No. of patient	Gender	Age	HA (mg/ml)	Clinical diagnosis
No.1	F	77	2.1	OA
No.2	M	70	1.9	OA
No.3	M	73	1.7	OA
No.4	M	47	2.2	TA
No.5	F	26	2.0	TA
No.6	F	30	1.7	TA

Fig. 6. (A) Effects of human synovial fluids on ALP activity in C2C12 cells, where the ALP activity is shown (control: cells not treated with synovial fluids; 1–6: cells treated with No. 1–No. 6 each synovial fluid). The asterisks indicate $P < 0.05$ compared with the control without any treatment. (B) Profiles of clinical synovial fluid samples (No. 1, No. 2, No. 3: osteoarthritis; No. 4, No. 5, No. 6: traumatic arthritis). The HA concentrations of all samples were measured in duplicates.

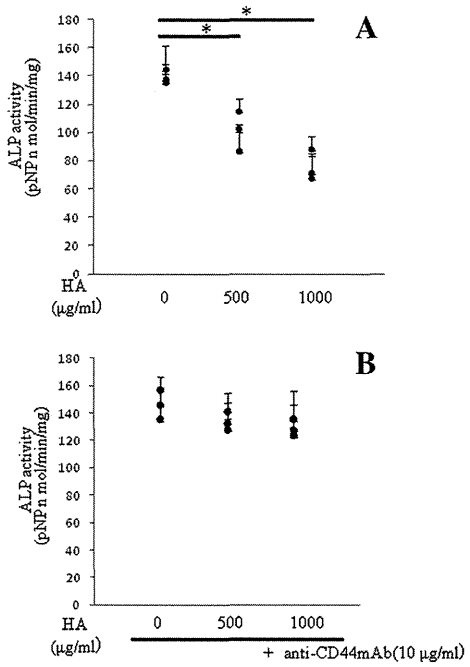

Fig. 7. Effects of hyaluronan (HA) on the alkaline phosphatase (ALP) activity levels in mouse calvaria cells. (A) Non-treated cells; (B) cells treated with 10 μg/ml CD44-blocking antibody. The data are the means ± S.D. based on three independent experiments performed using independent samples ($n = 3$). The asterisks indicate $P < 0.05$ compared with the control without any treatment.

Acknowledgments

We thank Mr. Morito Sakaue and Mr Hiroshi Fujita for their technical support. This study was supported by a Grant-in-Aid for Scientific Research (B) 23390363 from the Ministry of Education, Culture, Sports, Science, and Technology of Japan (K.N.).

Appendix A. Supplementary data

Supplementary data associated with this article can be found, in the online version, at http://dx.doi.org/10.1016/j.febslet.2014.12.031.

References

[1] Laurent, T.C. and Fraser, J.R. (1992) Hyaluronan. FASEB J. 6, 2397–2404.
[2] Lee, J.Y. and Spicer, A.P. (2000) Hyaluronan: a multifunctional, megaDalton, stealth molecule. Curr. Opin. Cell Biol. 12, 581–586.
[3] Entwistle, J. and Hall, C.L. (1996) HA receptors: regulators of signaling to the cytoskeleton. J. Cell. Biochem. 61, 569–577.
[4] Bourguignon, L.Y. (2008) Hyaluronan-mediated CD44 activation of RhoGTPase signaling and cytoskeleton function promotes tumor progression. Semin. Cancer Biol. 18, 251–259.
[5] Maharjan, A.S. and Pilling, D. (2011) High and low molecular weight hyaluronic acid differentially regulate human fibrocyte differentiation. PLoS ONE 6, e26078.
[6] Andhare, R.A. and Takahashi, N. (2009) Hyaluronan promotes the chondrocyte response to BMP-7. Osteoarthritis Cartilage 17, 906–916.
[7] Peterson, R.S. and Andhare, R.A. (2004) CD44 modulates Smad1 activation in the BMP-7 signaling pathway. J. Cell Biol. 166, 1081–1091.
[8] Chang, E.J. and Kim, H. (2007) Hyaluronan inhibits osteoclast differentiation via Toll-like receptor 4. J. Cell Sci. 120, 166–176.
[9] Huang, L. and Cheng, Y.Y. (2003) The effect of hyaluronan on osteoblast proliferation and differentiation in rat calvarial-derived cell cultures. J. Biomed. Mater. Res., Part A 66, 880–884.
[10] Wozney, J.M. (1995) The potential role of bone morphogenetic proteins in periodontal reconstruction. J. Periodontol. 66, 506–510.
[11] Takaoka, K. and Nakahara, H. (1988) Ectopic bone induction on and in porous hydroxyapatite combined with collagen and bone morphogenetic protein. Clin. Orthopedics Related Res. 234, 250–254.
[12] Nakase, T. and Nomura, S. (1994) Transient and localized expression of bone morphogenetic protein 4 messenger RNA during fracture healing. J. Bone Miner. Res. 9, 651–659.

Please cite this article in press as: Kaneko, K., et al. Hyaluronan inhibits BMP-induced osteoblast differentiation. FEBS Lett. (2015), http://dx.doi.org/10.1016/j.febslet.2014.12.031